the first 20 min of incubation, 23% of the particles were taken up by sperm cells. Later on, about 60% of these particles were released from the cells and a further linear uptake was observed for an additional 1.5 h of incubation. Particles were bound to the acrosome in the head of the sperm, and to mitochondria in the tail of the sperm. The sperm was further incubated for 4 h. Motility and the ability to undergo an acrosome reaction, i.e. the ability to fertilize an egg, were not affected by the presence of the magnetic nanoparticles.

2.1.5. Cobalt–chromium (CoCr) nanoparticles

Internal exposure to CoCr nanoparticles can occur by wear mechanism associated with metal-on-metal (CoCr) orthopaedic joint replacements [30]. An *in vitro* study of CoCr particles is presented in Table 3.

2.1.5.1. In vitro study of cobalt–chromium (CoCr) nanoparticles. The cellular toxicity of CoCr nanoparticles (29.5 ± 6.3 nm in diameter, Osprey Metals) when located on the other side of a fully confluent cellular barrier was assessed using BeWo b30 cells, a human trophoblast choriocarcinoma-derived cell line, which were grown as a multi-layered (3–4 cells thick) barrier to simulate tight barriers in the body like the placental barrier [30]. Human fibroblast cells were placed on one side of this layer of cells, and CoCr particles on the other. The fibroblasts were checked for DNA damage using the alkaline comet assay after introduction of the particles. Indirect exposure to CoCr nanoparticles caused DNA damage. Indirect exposure to micrometer-sized CoCr (2.9 ± 1.1 μm in diameter) also damaged DNA. More than 95% of the nanoparticles were located within the cells of the superficial layer after 24 h of exposure, indicating that nanoparticles were internalized by the BeWo cells and did not pass through the barrier. The authors of this paper noted that the DNA damage was mediated by a novel mechanism involving pannexin and connexin hemichannels and gap junctions and purinergic signaling. These findings suggest that there is some possibility of placental transfer of particles.

2.1.6. Silica (SiO_2)

Industrial silica products are widely used in the electronics industry and as a food additive, and nanosized amorphous silica is used in a wide variety of applications including catalytic supports, photonic crystals, gene delivery, photodynamic therapy, and biomedical imaging [31]. An *in vitro* study of silica particles is presented in Table 3.

2.1.6.1. In vitro study of silica (SiO_2). The embryonic stem (ES) cell test using the D3 murine ES cell line was performed to determine the potential of spherical amorphous silica nanoparticles (10, 30, 80 and 400 nm in average primary particle size, Glantreo Ltd.) to inhibit the differentiation of ES cells into spontaneously contracting cardiomyocytes [32]. Silica nanoparticles were dialyzed against pure MilliQ water and diluted in distilled water, and the ES cells were exposed at 1–100 μg/mL throughout the entire 10-day test period. Transmission electron microscopy revealed that the dried silica particles were spherical and showed no substantial aggregation, except for the 10 nm particles, and measured diameters of the particles specified as 10, 30, 80, and 400 nm by the manufacturer were 11, 34, 34, and 248 nm, respectively. Silica particles of 30, 80 and 400 nm were observed in cells of the embryonic body. A concentration-dependent inhibition of the differentiation of ES cells into contracting cardiomyocytes was observed after exposure to 10 and 30 nm particles while the 80 and 400 nm particles did not inhibit the differentiation at up to 100 μg/mL. The inhibitory effect of the 30 nm particles was greater than that of the 10 nm particles as evidenced by the estimated ID_{50} values, 29 and 59 μg/mL, respectively. Inhibition of the differentiation of ES cells occurred below cytotoxic concentrations, suggesting a specific effect of the 10 and 30 nm particles on the differentiation of the ES cells.

2.2. Fullerenes (C_{60})

A fullerene is any molecule entirely in the form of a hollow sphere, ellipsoid, or tube. The first fullerene to be discovered is known as buckminsterfullerene C_{60}. Fullerenes have unique physicochemical properties that have been exploited for use in cosmetics, lubricants, dietary supplements, building materials, clothing treatment, electronics, and fuel cells [33]. *In vivo* and *in vitro* studies on fullerenes are listed in Table 4.

2.2.1. In vivo study of fullerenes (C_{60})

[60]Fullerene (C_{60}, purity > 99.9%, Terms Co.) was solubilized with poly(vinylpyrrolidone) (PVP). Pregnant Slc mice (n = 2/group) were intraperitoneally injected with C_{60} at 25, 50, or 137 mg/kg, PVP, or distilled water on DG 10, and their embryos were examined 18 h after injection [34]. No effects were observed in embryos of dams injected with PVP or distilled water. After the injection of C_{60}, all embryos died at 137 mg/kg. At 50 mg/kg, C_{60} was clearly distributed into the yolk sac and embryos and 50% of embryos were abnormal in shape predominantly in the head and tail regions. At 25 mg/kg, one pregnant mouse had all normal embryos and the other had only one abnormal embryo. The authors of this study speculated that C_{60} was incorporated into the concepts and the severely disrupted the function of the yolk sac and embryonic morphogenesis.

The distribution of $[^{14}C]_{60}$ was determined in rat dams and their pre- and postnatal offspring [35]. C_{60}, with an average particle size of less than 10 nm and estimated at 2 nm, was suspended in PVP. SD rats were given an intravenous injection of a suspension of approximately 0.3 mg $[^{14}C]_{60}$/kg into the tail vein on GD 15 or lactational day (LD) 8, and tissues of dams were collected 24 h (n = 4) and 48 h (n = 3) later. In pregnant dams at 24 h after injection, radioactivity was found in the liver (43% of the injected radioactivity), spleen (4%), reproductive tract (3%), and placenta (2%). Radioactivity was also detected in the digest of fetuses (0.87%). In lactating dams, radioactivity was detected in the liver (35%), spleen (4%), reproductive tract (0.10–0.42%), mammary tissue (0.48–0.94%), and milk at 24 h after injection. Radioactivity transferred to pups via lactation was found in the gastrointestinal tract (0.28%) in pups sacrificed at 24 h after injection, with an increase in distribution to the gastrointestinal tract of pups (0.43%) by 48 h after injection. The authors of this study noted that C_{60} distributed to the placenta and fetuses of exposed pregnant dams and to the milk and pups of exposed lactating dams.

2.2.2. In vitro study of fullerenes (C_{60})

Midbrain tissue samples of embryos of pregnant Slc–ICR mice on GD 11 were dissociated into individual cells, cell suspensions were prepared in culture medium, and a midbrain micromass culture was performed to evaluate the toxicity of C_{60} solubilized with PVP [34]. The C_{60} solution in the medium was incorporated into the midbrain culture plates, and further cultured for 6 days. The IC_{50} values of C_{60} for cell differentiation and proliferation were 0.43 and 0.47 mg/mL, respectively. Differentiation was inhibited as cytotoxicity increased. C_{60} was assumed to decrease cell proliferation via active oxygen species, because cell proliferation inhibited by C_{60} was partly restored by the addition of antioxidative enzymes.

2.3. Carbon black (CB)

CB is a low solubility particle produced industrially from incomplete thermal decomposition of hydrocarbons, a process controlled

Table 4
In vivo and *in vitro* reproductive and developmental toxicity studies of fullerenes (C_{60}), carbon black (CB), cadmium selenium-core quantum dots (CdSeQDs) and polystyrene-based fluorescent particles.

In vivo/in vitro	Materials/characteristics	Animals/cells	Exposure			Findings	References
			Route/method	Duration/time	Concentration		
In vivo	C_{60} (purity > 99.9%)	Slc mice	Intraperitoneal injection	Single on GD 10	25–137 mg/kg	Deaths of all embryos at 138 mg/kg Abnormalities in 50% of embryos at 50 mg/kg	[34]
In vivo	[^{14}C]C_{60} (>10 nm, estimated 2 nm in particle size)	SD rats	Intravenous injection	Single on DG 15 or LD 8	Approx. 0.3 mg/kg (3–4 rats/group)	Distribution of C_{60} to placentae and fetuses of exposed pregnant dams Distribution of C_{60} to milk and offspring of exposed lactating dams	[35]
In vitro	C_{60} (purity > 99.9%)	Midbrain cells of Slc:ICR mouse embryos at GD 11	Incubation	6 days	10–1000 μg/mL	IC_{50} for cell differentiation = 430 μg/mL IC_{50} for cell proliferation = 470 μg/mL	[34]
In vivo	CB Printex 90 (14 nm in particle size, 300 m^2/g in surface area) Printex 25 (56 nm in particle size, 45 m^2/g in surface area) Flammruss 101 (95 nm in particle size, 20 m^2/g in surface area)	ICR mice	Intratracheal instillation	10 times at weekly intervals	0.1 mg/mouse	No effect of 14, 56 or 95 nm particles on body weight or reproductive organs ↑ Serum testosterone levels after instillation of 14 and 56 nm particles ↓ DSP after instillation of 14, 56, and 90 nm particles	[37]
In vitro	CB (14 nm in particle size, Printex 90)	Mouse testis Leydig cell line TM3	Incubation	16, 24, or 48 h	1–1000 μg/mL	↓ Viability of TM3 at 1000 μg/ml No effect on proliferation of TM3 cells No changes in HO-1 mRNA expression at up to 100 μg/mL ↑ StAR mRNA expression at 30 μg/mL for 48 h-incubation	[20]
In vitro	CdSeQDs (approx. 3.5 nm in diameter) ZnS coating CdSeQDs	ICR mouse morulas and blastocysts	Incubation	24 h	125, 250, or 500 nmol/L	↓ Development of morulas into blastocysts at 250 and 500 nmol/L ↑ Number of apoptotic cells of blastocysts at 250 and 500 nmol/L ↓ Cell proliferation of blastocysts at 250 and 500 nmol/L ↓ Blastocyst development at 125 nmol/L and higher No cytotoxicity of ZnS coating CdSeQDs	[38]
In vitro	CdSeQDs (approx. 3.5 nm in diameter)	Female ICR and male C57BL/6J mice	Blastocysts were preincubated with CdSeQDs and transfered to pseudopregnat mice	Preincubation of blastocysts for 24 h	500 nmol/L	↓ Implantation rate ↑ Resorptions ↑ Embryos with abnormal development ↓ Fetal weight	[38]
In vitro	Polystyrene-based fluorescent nanoparticles (microspheres 40 to over 120 nm in size, Molecular Probes Inc.)	Two-cell stage mouse embryos	Incubation	4 days for 2-cell embryos 48 h for blastocysts	11.0 million/mL	No effect on development of 2-cell embryos No effect on hatching, implantation, or degeneration after exposure up to the blastocyst stage	[41]

to achieve pre-defined and reproducible particle sizes and properties suitable for a diverse range of industrial applications [36]. The CB particles so formed are complex, with a degenerated graphitic crystallite structure and high-power electron micrographs clearly show irregular layered graphitic plates. The most common use of CB is as a pigment and reinforcing phase in automobile tires. CB helps conduct heat away from the tread and belt area of the tire, reducing thermal damage and increasing tire life. CB is also employed in some radar-absorbent materials and in photocopiers and laser printer toner. *In vivo* and *in vitro* studies of CB are listed in Table 4.

2.3.1. In vivo study of carbon black (CB)

The effect of CB nanoparticles with a primary size of 14 nm (300 m^2/g in surface area, Printex 90, Degussa), 56 nm (45 m^2/g in surface area, Printex 25, Degussa), and 95 nm (20 m^2/g in surface area, Flammruss 101, Degussa) on the male reproductive system was determined [37]. Six-week-old male ICR mice (n = 15–16/group) were intratracheally instilled with CB particles suspended in normal saline containing 0.05% Tween 80 at 0.1 mg/mouse for the 14, 56, and 95 nm CB particles and 1.56 μg/mouse for the 14 nm CB (particle number concentration of 14 nm CB is the same as that of 56 nm CB). Mice received 10 weekly instillations and were killed on day after the last instillation. No effect of the 14, 56, or 96 nm particles was observed on body weight or male reproductive organ weights. Vacuolation of the seminiferous tubules and decreased DSP were found in mice instilled with all three sizes of CB particles. Levels of serum testosterone were increased after instillation of all three particles. The group exposed to the 14 nm particles, with approximately the same number of particles per unit volume as the 56 nm particles, showed fewer effects than did the group exposed to the 56 nm particles. The authors noted that CB nanoparticles impaired the function of Leydig cells, and the consequent fluctuation of sperm testosterone levels caused a reduction of DSP. These findings suggest that CB nanoparticles adversely affect mouse spermatogenesis and the effect depends on particle mass rather than particle number.

2.3.2. In vitro study of carbon black (CB)

The direct effects of CB (14 nm in particle size, Printex 90, Degussa) on testis-constituent cells was determined using the mouse Leydig cell line TM3 [20]. The test was performed using the procedure described above in the TiO_2 section. The uptake of CB nanoparticles by Leydig cells was detected after 48 h. Cell viability was markedly inhibited at 1000 μg/mL, but CB did not affect the proliferation of TM3 cells. No effect of CB was found on the expression of HO-1 mRNA in TM3 cells at up to 100 μg/mL. StAR mRNA expression was increased at 30 μg/mL after incubation for 48 h. These findings suggest that CB nanoparticles have no direct effect on the induction of oxidative stress but affect the production of steroid hormones in Leydig cells.

2.4. Luminescent particles

In vitro studies of cadmium selenium-core quatum dots (CdSeQDs) and polystyrene-based fluorescent particle have been published.

2.4.1. Cadmium selenium-core quantum dots (CdSeQDs)

Quantum dots are colloidal nanocrystalline semiconductors that have unique light-emitting properties and can be used as a novel luminescent material [38]. CdSeQDs are useful as an alternative to fluorescent dyes for use in biological imaging, due to their bright fluorescence, narrow emission, broad UV excitation, and high photostability [39]. An *in vitro* study of CdSeQDs is shown in Table 4.

2.4.1.1. In vitro study of cadmium selenium-core quantum dots (CdSeQDs). The developmental effect of CdSeQDs (approximately 3.5 nm in diameter) was determined using mouse embryos [38]. For water solubilization, the CdSeQDs were surface coupled with mercaptoacetic acid and suspended in PBS. Morulas and blastocysts were obtained from superovulating ICR female mice, which were mated with fertile males of the same strain, by flushing the fallopian tubes on GD 3 and flushing the uterine horns on GD 4, respectively. After incubation of morulas or blastocysts with CdSeQDs for 24 h, an inhibition of the preimplantation development of morulas into blastocysts, increased number of apoptotic cells in the inner cell mass (ICM) of blastocysts (n = 200/group) and inhibition of cell proliferation, primarily in the ICM, of blastocysts (n = 180/group) at 250 nmol/L and above, and inhibition of the postimplantation development of blastocysts at 125 nmol/L and above were observed. To examine the effect of CdSeQDs on the piostimplantation development of blastocysts, blastocysts (n = 200/group) exposed to 0 or 500 nmol/L for 24 h were transferred to recipient ICR mice (n = 25/group), which were mated with vasectomized C57BL/6J male mice, on pseudopregnant day (PD) 4 and killed on PD 18. A decreased implantation rate and fetal weight, and increased numbers of embryos with abnormal development and resorptions were observed in the CdSeQDs-treated group. CdSeQDs coated with ZnS had no significant cytotoxic effect on blastocyst development. These findings indicate that CdSeQDs affect adversely pre- and postimplantation embryonic survival and development and the ZnS coating alters the CdSeQD-induced toxicity.

2.4.2. Polystyrene-based fluorescent particles

Fluorescent nanoparticles are promising tools for optical data storage and other technical applications in biochemical, bioanalytical, and medical areas, and were successfully used for immunoassays [40]. An *in vitro* study of fluorescent nanoparticles is shown in Table 4.

2.4.2.1. In vitro study of polystyrene-based fluorescent particles. The effect of ultrafine polystyrene-based fluorescent particles (Molecular Probes Inc.), ranging from 40 nm to over 120 nm in size with different fluorescence colors corresponding to particle size, on mouse embryos was examined [41]. Two-cell stage embryos were incubated with fluorescent nanoparticles at 11.0 million/mL for 4 days, and development was assessed. Untreated embryos incubated for 4 days were further incubated with fluorescent nanoparticles at 11.0 million/mL for 48 h, and the developmental stages of the blastocysts were assessed. No effect of nanoparticles was found on the development of 2-cell stage embryos to the blastocyst stage. There was no effect of nanoparticles on hatching, implantation on the culture dish, or degeneration after additional exposure until the blastocyst stage. Although nanoparticles were internalized, the development of embryos was not affected. Nanoparticles were predominantly found in the trophoblast cells with a few located in the inner cell mass in hatched blastocysts. These findings show that fluorescent nanoparticles did not affect the development of mouse early embryos and suggest that internalized nanoparticles did not affect cellular processes or the expression of factors needed for development.

3. Discussion and conclusions

This paper reviewed the *in vivo* and *in vitro* studies on the reproductive and developmental toxicity of nanomaterials. Although it provides initial information on the potential toxicity of nanomaterials, it should be followed up by relevant hazard studies of nanomaterials.

In vivo studies have showed increased allergic susceptibility in offspring of mouse dams intranasally insufflated with respirable-

size TiO_2, adverse effects on spermatogenesis and histopathological changes in the testes, and changes in gene expression in the brain in mouse offspring after maternal subcutaneous injections of TiO_2 nanoparticles, transfer to rat fetuses of radiolabeled gold nanoparticles and C_{60} after maternal intravenous injection, death and morphological abnormalities in mouse embryos after maternal intraperitoneal injections of C_{60}, and adverse effects on spermatogenesis in mouse offspring after maternal intratracheal instillations of CB nanoparticles. However, these studies were performed with 1–10 administrations of a large bolus and/or a route of exposure not relevant to humans using relatively small numbers of animals. *In vivo* studies should be performed that include doses that closely reflect expected exposure levels. Major routes of exposure to nanoparticles are the respiratory tract, skin, eyes, and gastrointestinal tract. Studies using relevant routes of exposure are needed to clarify the toxicity of nanoparticles. The number of animals per group should be sufficient to allow meaningful interpretation of the data for reproductive and developmental toxicity studies, and a dose–response analysis is also needed to allow more realistic comparisons with actual human exposure. In the studies presented in this review paper, there was a lack of information regarding maternal toxicity. The investigation of maternal toxicity is essential for reproductive and developmental toxicity studies, because the toxicity to offspring may be modified or influenced by toxicity to the mother, and toxicity to offspring often occurs in conjunction with maternal toxicity in animal studies.

Radioactivity was detected in rat fetuses of dams intravenously injected with gold nanoparticles or C_{60}, but unlabeled gold nanoparticles were not detected in mouse fetuses of dams injected intravenously or in the fetal outflow of human placenta. *In vitro* study also revealed some possibility of placental transfer of CoCr particles mediated by a novel mechanism. In terms of developmental toxicity, information on the placental transfer of nanomaterials to offspring of dams given during gestation and lactation is of great interest in interpretation of the data. Measurements of the placental transfer of nanoparticles are an important source of information on the mechanism of action and the risk of nanoparticles, and may help to clarify the reproductive and developmental toxicity of nanoparticles.

As for the effect of nanoparticles on embryonic development, maternally administered C_{60} impaired embryonic development and the results of micromass culture suggest a dysmorphogenic effect of C_{60}. The C_{60} was clearly distributed into the yolk sac. These findings resemble those of developmental toxicity studies of trypan blue, which was teratogenic in mice, rats, hamsters, and guinea pigs [42]. It is generally accepted that teratogenic action of trypan blue in rats is due to its accumulation and interference in the function of the yolk sac, an organ of histotrophic nutrition that provides the principal source of nutrients before the initiation of functional chorio-allantoic placentae. Mice and rats have a yolk sac placenta, which plays a significant role during early in organogenesis. This is not the case for humans and monkeys in which the yolk sac placenta is of insignificant importance. Trypan blue produces malformations in rats and mice due to its accumulation in the yolk sac. This is not possible in humans and monkeys [43].

It is noted that test conducted and reported according to international accepted test guidelines and in compliance with the principles of Good Laboratory Practice (GLP) should have the highest grade of reliability and data for hazard identification must be evaluated considering their quality and adequacy for risk assessment [44]. At present, however, such studies are not available for reproductive and developmental toxicity of nanomaterials. Oberdörster et al. [1] described that studies to assess reproductive effects following pulmonary exposure to nanomaterials should follow protocols similar to OECD guideline 422 for the Testing of Chemicals (Combined Repeated Dose of Toxicity Study with the Reproduction/Developmental Toxicity Screening Test). The OECD guideline 421 for Testing of Chemicals (Reproduction/Developmental Toxicity Screening Test) is also useful to obtain initial information on possible effects on reproduction and development. In these tests, test materials are given to male rats for a minimum of 4 weeks beginning before mating and to females beginning before mating to shortly after parturition of pups. These screening tests are performed using relatively small numbers of animals in the dose groups and do not provide complete information on all aspects of reproduction and development due to the limitation of the exposure period and selectivity of endpoints. The two-generation study, which covers the whole reproductive cycles of at least one generation, may be adequate to evaluate the reproductive and developmental toxicity of nanomaterials. However, the concentrations, populations, and duration of exposure to nanomaterials are different from one another. It is required to modify the exposure period and the endpoints correlated with the exposure period. To further evaluate the reproductive and developmental toxicity of nanomaterials, a more specific test should be designed on a case-by-case basis according to the characterization of human exposure.

In vitro studies revealed high concentrations of TiO_2 nanoparticles to affect the viability and proliferation of mouse Leydig cells, but not the gene expression associated with spermatogenesis. Gold nanoparticles decreased the motility of human sperm, silver, aluminum, and MoO_3 were toxic to mouse spermatogonia stem cells, CoCr nanoparticles damaged DNA of human fibroblast cells, silica nanoparticles inhibited the differentiation of mouse ES cells, C_{60} inhibited the differentiation of mouse midbrain cells, CB decreased the viability of mouse Leydig cells, and CdSeQDs inhibited the pre- and postimplantation development of mouse embryos. In these studies, the concentrations of nanoparticles were very high and unlikely to occur in animal studies. The mechanistic pathways that operate at low realistic concentrations are likely to be different from those operating at very high concentrations when the cell's or organism's defenses are overwhelmed [2]. The findings of these *in vitro* studies are difficult to evaluate because of differences in the chemical composition and sizes of particles, target cells, duration of exposure, endpoints, and exposure concentrations among experiments. *In vivo* studies correlated with results obtained from *in vitro* studies should be performed.

Oxidative stress as a common mechanism for cell damage induced by nanoparticles is well known and a wide range of nanomaterial species have been shown to create reactive oxygen species (ROS) both *in vivo* and *in vitro*. It is suggested that a free radical-induced mechanism or another form of oxidative stress played a role in the developmental toxicity of C_{60} in zebrafish, in which C_{60} caused decreases in the embryonic survival rate, the hatching rate, heartbeat and pericardial edema, and the toxicity was effectively attenuated by adding glutathione, an antioxidant [45]. In mammals, TiO_2 nanoparticles in Leydig cells, Sertili cells, spermatids, and cells of the olfactory bulb and cerebral cortex of pups, and C_{60} in embryos and yolk sac were noted after a maternal administration. In *in vitro* studies, TiO_2 and CB nanoparticles in Leydig cells, Fe_3O_4 and gold nanoparticles in sperm cells, silica nanoparticles in cells of the embryonic body, CoCr nanoparticles in BeWo cells, and fluorescent nanoparticles in trophoblast cells were observed. Determination of the oxidative stress in these cells may help us to understand the reproductive and developmental toxicity of nanoparticles.

The contradicting results obtained from the studies presented in this review may be attributed to the use of different nanomaterials and experimental models, the exposure during different stages of offspring development, and evaluations with different endpoints. It is likely that the size, shapes, chemistry, crystallinity, surface properties, concentration, agglomeration, and dose of nanoparticles are all involved in detecting biological activity. The characterization of

administered materials in toxicity studies is fundamental, and characterizing delivered nanomaterials after administration in a test system or model provides the best quality data on dose and material properties that are related to observed responses, but this is limited by current methodological capabilities [2]. Further studies, especially *in vivo*, using different types of characterized materials, relevant routes of administration, and doses closely reflecting expected levels of exposure are needed to adequately evaluate the reproductive and developmental toxicity of nanomaterials.

Conflict of interest

None.

Acknowledgements

This study was conducted under the "Evaluating Risks Associated with Manufactured Nanomaterials" Project funded by the New Energy and Industrial Technology Development Organization (NEDO), Japan.

References

[1] Oberdörster G, Maynard A, Donaldson K, Castranova V, Fizpatric J, Ausman K, et al. Principles for characterizing the potential human health effects from exposure to nanoparticles: elements of a screening strategy. Part Fibre Toxicol 2005;2:8, doi:10.1186/1743-8977-2-8.
[2] Oberdörster G, Oberdörster E, Oberdörster J. Nanotoxicology: an emerging discipline evolution from studies of ultrafine particles. Environ Health Perspect 2005;113:823–39.
[3] Penn SG, He L, Natan MJ. Nanoparticles for bioanalysis. Curr Opin Chem Biol 2003;7:609–15.
[4] Liu WT. Nanoparticles and their biological and environmental applications. J Biosci Bioeng 2006;102:1–7.
[5] Colborn T, vom Saal F, Soto A. Developmental effects of endocrine-disrupting chemicals in wildlife and humans. Environ Health Perspect 1993;101:378–84.
[6] Brooking J, Davis SS, Illum L. Transport of nanoparticles across the rat mucosa. J Drug Target 2001;9:267–79.
[7] Wang J, Liu Y, Jiao F, Lao F, Li W, Gu Y, et al. Time-dependent translocation and potential impairment on central nervous system by intranasally instilled TiO_2 nanoparticles. Toxicology 2008;254:82–90.
[8] Lee KP, Trochimowicz HJ, Reinhardt CF. Pulmonary response of rats exposed to titanium dioxide (TiO_2) by inhalation for two years. Toxicol Appl Pharmacol 1985;79:179–92.
[9] Lindenschmidt RC, Driscoll KE, Perkins MA, Higgins JM, Maurer JK, Belfiore KA. The comparison of a fibrogenic and two nonfibrogenic dusts by bronchoalveolar lavage. Toxicol Appl Pharmacol 1990;102:268–81.
[10] Muhle H, Bellmann B, Creutzenberg O, Dasenbrock C, Ernst H, Kilpper R, et al. Pulmonary response to toner upon chronic inhalation exposure in rats. Fundam Appl Toxicol 1991;17:280–99.
[11] Warheit B, Sayes CM, Reed KL, Swain KA. Health effects related to nanoparticle eposures: environmental, health and safety considerations for assessing hazards and risks. Pharmacol Ther 2008;120:35–42.
[12] Heinrich U, Fuhst R, Rittinghausen S, Cretzenberg O, Bellmann B, Koch W, et al. Chronic inhalation exposure of Wistar rats and two different strains of mice to diesel engine exhaust, carbon black, and titanium dioxide. Inhal Toxicol 1995;7:533–56.
[13] Baan R, Staif K, Grosse Y, Secretan B, Ghissassi F, Cogliano V, on behalf of the WHO International Agency for Research on Cancer Monograph Working Group. Carcinogenicity of carbon black, titanium dioxide, and talk; 2006 [cited June 22, 2009], available from: http://oncology.thelancet.com.
[14] Landsiedel R, Kapp MD, Schulz M, Wiench K, Oesch F. Genotoxicity investigations on nanomaterials: methods, preparation and characterization of test material, potential artifacts and limitations-many questions, some answers. Mutat Res 2009;681:241–58.
[15] Ema M, Kobayashi N, Naya M, Hanai S, Nakanishi J. Genotoxicity evaluation of titanium dioxide nanoparticles. Jpn J Environ Toxicol 2009;12:71–84 [in Japanese].
[16] Fedulov AV, Leme A, Yang Z, Dahl M, Lim R, Mariani TJ, Kobzik L. Pulmonary exposure to particles during pregnancy causes increased neonatal asthma susceptibility. Am J Respir Mol Biol 2008;38:57–67.
[17] CEPA/OEHHA (California Environmental Protection Agency/Office of Environmental Health Hazard Assessment). Safe drinking water and toxic enforcement ACT of 1986 (Position 65). Notice to interested parties, February 21, 2003. Chemical listed effective February 21, 2003 as known to the State of California to cause cancer; 2003 [cited October 13, 2009], available from: http://oehha.ca.gov/prop65/prop65_list/files/22103not.pdf.
[18] Shimizu M, Tainaka H, Oba T, Mizuo K, Umezawa M, Takeda K. Maternal exposure to nanoparticle titanium dioxide during the prenatal period alters gene expression related to brain development in the mouse. Part Fibre Toxicol 2009;6:20, doi:10.1186/1743-8977-6-20.
[19] Takeda K, Suzuki K, Ishihara A, Kubo-Irie M, Fujimoto R, Tabata M, et al. Nanoparticles transferred from pregnant mice to their offspring can damage the genital and cranial nerve system. J Health Sci 2009;55:95–102.
[20] Komatsu T, Tabata M, Kubo-Irie M, Shimizu T, Suzuki K, Nihei Y, et al. The effects of nanoparticles on mouse testis Leydig cells *in vitro*. Toxicol in Vitro 2008;22:1825–31.
[21] Shelley SA. Nanotechnology: turning basic science into reality. In: Theodore L, Kunz RG, editors. Nanotechnology-environmental implications and solution. Hoboken: John Wiley and Sons, Inc. Publication; 2005. p. 61–107.
[22] Challier JC, Panigel M, Meyer E. Uptake of colloidal ^{198}Au by fetal liver in rats, after direct intrafetal administration. Int J Nucl Med Biol 1973;1:103–6.
[23] Takahashi S, Matsuoka O. Cross placental transfer of ^{198}Au-colloid in near term rats. J Radiat Res 1981;22:242–9.
[24] Sadauskas E, Wallin H, Stoltenberg M, Vogel U, Doering P, Larsen A, et al. Kupper cells are central in the removal of nanoparticles from the organism. Part Fibre Toxicol 2007;4:10, doi:10.1186/1743-8977r-r4-10.
[25] Myllynen P, Loughran MJ, Howard CV, Sormunen R, Walsh A, Vähäkangas KH. Kinetics of gold nanoparticles in the human placenta. Reprod Toxicol 2008;26:130–7.
[26] Wiwantitkit V, Sereemaspun A, Rojanathanes R. Effect of gold nanoparticles on spermatozoa: the first world report. Fertil Steril 2009;91:e7–8.
[27] Kim WS, Kim HC, Hong SH. Gas sensing properties of MoO_3 nanoparticles synthesized by solvothermal method. J Nanopart Res 2009, doi:10.1007/s11051-009-9751-6.
[28] Braydich-Stolle L, Hussain S, Schlager JJ, Hofmann MC. *In vitro* cytotoxicity of nanoparticles in mammalian germline stem cells. Toxicol Sci 2005;88:412–9.
[29] Makhluf SBD, Qasem R, Rubinstein S, Gedanken A, Breibart H. Loading magnetic nanoparticles into sperm cells does not affect their functionality. Langmuir 2006;22:9480–2.
[30] Bhabra G, Sood A, Fisher B, Cartwright L, Saunders M, Evans WH, et al. Nanoparticles can cause DNA damage across a cellular barrier. Nat Nanotechnol 2009;4:876–83.
[31] Lin YS, Haynes CL. Impact of mesoporous silica nanoparticle size, pore ordering, and pore integrity on hemolytic activity. J Am Chem Soc 2010;132:4834–42.
[32] Park MVDZ, Annema W, Salvati A, Lesniak A, Elsaesser A, Barnes C, et al. In vitro developmental toxicity test detects inhibition of stem cell differentiation by silica nanoparticles. Toxicol Appl Pharmacol 2009;240:108–16.
[33] Loutfy RO, Lowe TP, Moravsky AP, Katagiri S. Commercial production of fullerenes and carbon nanoparticles. In: Perspectives of fullerene nanotechnology. Netherlands: Springer; 2002. p. 35–46.
[34] Tsuchiya T, Oguri I, Yamakoshi YN, Miyata N. Novel harmful effects of [60]fullerene on mouse embryos in vitro and in vivo. FEBS Lett 1996;393:139–45.
[35] Sumner SCJ, Fennell TR, Snyder RW, Taylor GF, Lewin AH. Distribution of carbon-14 labeled C_{60}($[^{14}C]C_{60}$) in the pregnant and in the lactating dam and the effect of C_{60} exposure on the biochemical profile of urine. J Appl Toxicol 2009, doi:10.1002/jat.1503.
[36] Donaldson K, Tran L, Jimenez LA, Duffin R, Newby DE, Mils N, et al. Combustion-derived nanoparticles: a review of their toxicology following inhalation exposure. Part Fibre Toxicol 2005;2:10, doi:10.1186/1743-89772-2-10.
[37] Yoshida S, Hiyoshi K, Ichinose T, Takano H, Oshio S, Sugawara I, et al. Effect of nanopaticles on the male reproductive system of mice. Int J Andol 2008;32:337–42.
[38] Chan WH, Shiao NH. Cytotoxic effect of CdSe quantum dots on mouse embryonic development. Acta Pharmacol Sin 2008;28:259–66.
[39] Derfus AM, Chan WCW, Bhatia SN. Probing the cytotoxicity of semiconductor quantum dots. Nano Lett 2004;4:11–8.
[40] Bangs LB. New developments in particle-based immunoassays: introduction. Pure Appl Chem 1996;68:1873–9.
[41] Bosman SJ, Niet SP, Patton WC, Jacobson JD, Corselli JU, Chan PJ. Development of mammalian embryos exposed to mixed-size nanoparticles. Clin Exp Obst Gyn 2005;32:222–4.
[42] Shepard TH, Lemire RJ. Catalog of teratogenic agents. 11th ed. Baltimore: The Johns Hopkins University Press; 2004.
[43] Nielsen E, Thorup I, Schnipper A, Hass U, Meyer O, Ladefoged J, et al. Children and the unborn child. Exposure and susceptibility to chemical substances—an evaluation. Environmental project No. 589, Miljøproject; 2001 [cited October 18, 2009], available from: http://www2.mst.dk/udgiv/Publications/2001/87-7909-574-7/pdf/87-7909-333-7.pdf.
[44] Klimisch HJ, Andreae M, Tillmann U. A systemic approach for evaluating the quality of experimental toxicological and ecotoxicological data. Regl Toxicol Pharmacol 1997;25:1–5.
[45] Zhu X, Zhu L, Li Y, Duan Z, Chen W, Alvarez PJJ. Developmental toxicity in zebrafish (*Danio retio*) embryos after exposure to manufactured nanomaterials: buckminsterfullerene aggregates (nC_{60}) and fullerol. Environ Toxicol Chem 2007;26:976–9.

Toxicology 276 (2010) 143–153

Contents lists available at ScienceDirect

Toxicology

journal homepage: www.elsevier.com/locate/toxicol

Biological response and morphological assessment of individually dispersed multi-wall carbon nanotubes in the lung after intratracheal instillation in rats

Norihiro Kobayashi[a,*], Masato Naya[a], Makoto Ema[a], Shigehisa Endoh[b], Junko Maru[b], Kohei Mizuno[c], Junko Nakanishi[a]

[a] Research Institute of Science for Safety and Sustainability, National Institute of Advanced Industrial Science and Technology, 16-1 Onagawa, Tsukuba, Ibaraki 305-8569, Japan
[b] Research Institute for Environmental Management Technology, National Institute of Advanced Industrial Science and Technology, Ibaraki 305-8569, Japan
[c] Metrology Institute of Japan, National Institute of Advanced Industrial Science and Technology, Ibaraki 305-8563, Japan

ARTICLE INFO

Article history:
Received 19 June 2010
Received in revised form 30 July 2010
Accepted 30 July 2010
Available online 7 August 2010

Keywords:
Multi-wall carbon nanotubes (MWCNTs)
Nanomaterial
Pulmonary toxicity
Intratracheal instillation

ABSTRACT

Biological responses of multi-wall carbon nanotubes (MWCNTs) were assessed after a single intratracheal instillation in rats. The diameter and median length of the MWCNTs used in this study were approximately 60 nm and 1.5 μm, respectively. Groups of male Sprague–Dawley rats were intratracheally instilled with 0.04, 0.2, or 1 mg/kg of the individually dispersed MWCNT suspension. After instillation, the bronchoalveolar lavage fluid was assessed for inflammatory cells and markers, and the lung, liver, kidney, spleen, and cerebrum were histopathologically evaluated at 3-day, 1-week, 1-month, 3-month, and 6-month post-exposure. Transient pulmonary inflammatory responses were observed only in the lungs of the group of rats exposed to 1 mg/kg of MWCNTs. Morphology of the instilled MWCNTs in the lungs of rats was assessed using light microscopy and transmission electron microscopy (TEM). Light microscopy examination revealed that MWCNTs deposited in the lungs of the rats were typically phagocytosed by the alveolar macrophages and these macrophages were consequently accumulated in the alveoli until 6-month post-exposure. The 400 TEM images obtained showed that all MWCNTs were located in the alveolar macrophages or macrophages in the interstitial tissues, and MWCNTs were not located in the cells of the interstitial tissues. There was no evidence of chronic inflammation, such as angiogenesis or fibrosis, induced by MWCNT instillation. These results suggest that MWCNTs were being processed and cleared by alveolar macrophages.

1. Introduction

Carbon nanotubes (CNTs) are fiber-shaped substances that consist of graphite hexagonal-mesh planes (graphene sheet) present as a single-layer or as multi-layers with nest accumulation. Tubes with single-wall structures and multi-wall structures are called single-wall carbon nanotubes (SWCNTs) and multi-wall carbon nanotubes (MWCNTs), respectively. CNTs are regarded as nanomaterials because their diameters are within the nanoscale range (1–100 nm). Currently, various applied studies are focusing on CNTs because of their excellent physical–chemical properties.

However, there is a growing concern regarding the hazards of CNTs. Many pulmonary toxicity studies (e.g., inhalation exposure studies, intratracheal instillation studies, and pharyngeal aspiration studies) have reported that multifocal granulomas or fibrotic responses were persistently observed in the lungs of rats and mice after SWCNT exposure (Warheit et al., 2004; Lam et al., 2004; Mangum et al., 2006; Chou et al., 2008; Miyawaki et al., 2008; Shvedova et al., 2005, 2007, 2008a,b). MWCNT pulmonary toxicity studies also reported similar pulmonary responses as SWCNT exposure. Granulomatous inflammation and fibrotic responses were reported in MWCNT inhalation exposure studies (Muller et al., 2005; Li et al., 2007; Ma-Hock et al., 2009; Pauluhn, 2010).

The major concerns of CNT toxicity are that those objects are nanoscaled, and more importantly, they are fiber-shaped (i.e., they may have asbestos-like properties). Takagi et al. (2008) reported that most p53+/− transgenic mice died owing mesothelioma up to 180 days after intraperitoneal injection of MWCNTs at a dose of 3 mg/mouse (approximately 100 mg/kg body weight). Poland et al. (2008) reported that inflammatory responses were observed in mice exposed to fibers longer than 15 μm, but not in those exposed to shorter fibers, at 1 and 7 days after intraperitoneal injection of MWCNTs, asbestos, or carbon black particles at 50 μg/mouse. In a more recent intraperitoneal injection study with MWCNTs, however, there was no significant increase in the incidence of mesothelioma at doses of 2 and 20 mg/rat, even 2 years after injec-

* Corresponding author. Tel.: +81 29 861 8742; fax: +81 29 861 8415.
E-mail address: norihiro-kobayashi@aist.go.jp (N. Kobayashi).

0300-483X/$ – see front matter © 2010 Elsevier Ireland Ltd. All rights reserved.
doi:10.1016/j.tox.2010.07.021

tion, although the incidence of mesothelioma was significantly increased after administration of crocidolite (Muller et al., 2009).

In most CNT toxicity studies, CNT agglomerates were used as the test samples. However, some studies indicate that dispersed CNTs are more toxic than agglomerated CNTs when inhaled or instilled into the lungs of experimental animals. Muller et al. (2005) reported that MWCNT samples ground by a ball mill induced greater inflammation than non-ground bulk MWCNT samples after intratracheal instillation in rats. In their reports, the average length of the MWCNT samples was greatly decreased from 5.9 to 0.7 μm because of the ball mill grounding; but major characteristics such as the diameter or surface area did not change. Mercer et al. (2008) reported that after pharyngeal aspiration exposure of mice to dispersed SWCNTs (average particle size, 0.69 μm) and non-dispersed SWCNTs (average particle size, 15.2 μm), thickening of the alveolar walls was observed only in the group exposed to dispersed SWCNTs. Mercer et al. (2008) concluded that the dispersed SWCNTs were rapidly incorporated into the alveolar interstitium. Porter et al. (2010) suggested that the dispersed MWCNTs could reach the pleura after pharyngeal aspiration exposure in mice. These findings indicate that toxicity studies using agglomerated CNTs are inadequate to evaluate the hazards and risks of CNTs. However, there are few toxicity studies with dispersed CNTs. Further, there is little information regarding the behavior of MWCNTs after deposition in the lungs.

There are many potential applications of MWNCTs (e.g., in electrically conducting ceramics, anti-static clothing, and heat-exchange materials, etc.). To explore these applications, MWCNT dispersion is a key factor. Extensive research on MWCNT dispersion is underway in several organizations. Therefore, it is possible that exposures to dispersed MWCNTs might occur in the near future, necessitating the evaluation of the hazards of exposure to dispersed MWCNTs.

In this study, individually dispersed MWCNTs were intratracheally instilled in rats, and the biological responses (e.g., pulmonary inflammation) were assessed. Further, light microscopic and transmission electron microscopic examinations were performed to evaluate the behavior of MWCNTs in the lungs.

2. Materials and methods

2.1. Sample preparation

MWCNT samples (MWNT-7, Lot#T050831-01) were purchased from Mitsui & Co. Ltd. (Tokyo, Japan). MWNT-7 is a highly pure MWCNT sample, in which the carbon content is 99.79% (determined by fluorescence X-ray analysis). MWNT-7 has been used in many toxicity studies such as those by Takagi et al. (2008) and Poland et al. (2008). MWNT-7 is produced as a dry powder and the tubes do not aggregate together. To disperse MWCNTs in liquid for intratracheal instillation, MWCNTs (0.04, 0.2, or 1 mg/mL) and a maximum of 10 mg/mL of polyoxyethylene sorbitan monooleate (Tween 80, Wako Pure Chemical Industries, Ltd., Osaka, Japan) were added to Milli-Q water (Millipore Corporation, Billerica, MA, USA) and then ultrasonicated using an ultrasonic bath (5510J-MT, Branson Ultrasonics Div. of Emerson Japan, Ltd., Kanagawa, Japan) for 90 min at 135 W and a frequency of 42 kHz. PBS (10 mM) was then added to the ultrasonicated MWCNT suspension. The above MWCNT suspensions were used for intratracheal instillation the day after their preparation.

Tween 80 (10 mg/mL) in PBS (10 mM) was used as the negative (vehicle) control. Min-U-Sil 5 crystalline silica particles (US Silica Co., Berkley Springs, WV, USA), which produce continuous pulmonary inflammation in the lungs of rats with 5 mg/kg of intratracheal instillation (Warheit et al., 2006, 2007a,b; Kobayashi et al., 2009), was used as the positive control and was prepared as described for the MWCNT suspension. The concentration of the crystalline silica particles was adjusted to 5 mg/mL for intratracheal instillation.

2.2. MWCNT characterization

For both the bulk MWCNT samples and MWCNT suspensions, the agglomeration state and fiber length were evaluated based on observation using a scanning electron microscope (SEM) (SM-5410, JEOL Ltd., Tokyo, Japan) and a transmission electron microscope (TEM) (TM-1010, JEOL Ltd., Tokyo, Japan).

The BET surface area was measured by the N_2-adsorption method using Autosorb (Quantachrome Instrument, Boynton Beach, FL, USA) at a pressure ranging from 10.3 to 31.4 kPa. Purity of the MWCNT samples was measured by thermogravimetric analysis (TGA) using an auto simultaneous TG/DTA instrument (DTG-60H, Shimadzu Corporation, Kyoto, Japan). Furthermore, presence of defects in the graphene structure of the bulk MWCNT samples and the MWCNT suspensions was evaluated by Raman spectroscopy analysis (Nicolet Almega XR micro-Raman system, Thermo Fisher Scientific Inc., Japan). The resonance Raman scattering spectra were measured in the frequency regions of 100–3000 cm^{-1} with excitation wavelength at 532 nm.

The MWCNT suspension was characterized within 1 week of sample preparation. This is because we had monitored the time-dependent changes in the agglomeration state of the MWCNTs in the suspension using laser diffraction (Helos, Sympatec, Clausthal-Zellerfeld, Germany), and no significant difference was noted in the equivalent diameters of MWCNTs within 1 week of sample preparation.

2.3. Experimental animals

In this study, 8-week-old male Crl:CD(SD) rats (Charles River Laboratories Japan, Inc., Yokohama, Japan) were used. The rats were kept in an animal facility and housed in positive-pressure air-conditioned units (21–24 °C, 42–64% relative humidity) with 12 h light and dark cycles. After a 7-day acclimation, the body weight of each rat was measured and assigned to the study. Their body weight was in the range of 288–336 g at intratracheal instillation.

2.4. General experimental design

Rats were anesthetized with ether, and 1 mL/kg body weight of MWCNTs, negative control, or the positive control (crystalline silica particle) suspension were instilled into the trachea using a 18G indwelling needle, corresponding to doses of 0.04, 0.2, or 1 mg/kg body weight of MWCNTs and 5 mg/kg body weight of crystalline silica particles. Following instillation, the viability and general condition of the rats were observed once a day until dissection. The body weight of each rat was measured before instillation and at 1-, 3-, 7-, 14-, 21-, 28-, 35-, 42-, 49-, 56-, 63-, 70-, 77-, 84-, and 91-day post-exposure. Measurements of the organ weight of the left lung, bronchoalveolar lavage fluid (BALF) examination from the right lung, and histopathological evaluation of the left lung, liver, kidney, spleen, and cerebrum were performed at 3-day, 1-week (7 days), 1-month (28 days), and 3-month (91 days) post-exposure. Five rats per group were evaluated at each time point.

Animal experiments were performed in 2009 at the Kashima Laboratory, Mitsubishi Chemical Medience Corp. (Tokyo, Japan) in accordance with the Law for Partial Amendments to the Law Concerning the Protection and Control of Animals (2005). This study was approved by the Institutional Animal Care and Use Committee of the Testing Facility and performed in accordance with the ethics criteria contained in the bylaws of the Committee of National Institute of Advanced Industrial Science and Technology.

2.5. Bronchoalveolar lavage

The rats were euthanized by administrating an intraperitoneal injection of pentobarbital sodium (Nembutal injectable, Dainippon Sumitomo Pharma Co., Ltd., Tokyo, Japan) followed by exsanguination. The left bronchus was clamped with forceps, and the right bronchus was cannulated. Subsequently, 3 mL of heated (~37 °C) saline (Otsuka Pharmaceutical Factory, Inc., Tokushima, Japan) was instilled and aspirated to and from the lung to recover the first BALF fraction (approximately 2 mL). The supernatant was obtained by centrifuging the BALF at 300 g for 5 min and was used for the biochemical and cytokine measurements. Thereafter, 2 mL of saline solution was instilled and aspirated to and from the lung twice, and then additional BALF (approximately 4 mL) was obtained, centrifuged at 300 g for 5 min after addition to the precipitation obtained by centrifugation of the first BALF. The cell fraction was used to determine cell counts in the BALF.

2.6. Pulmonary cell counts

The cell fractions were suspended in saline with addition of BSA (0.1%) and EDTA-2K (0.05 mM) dissolved in PBS, and the number of total cells, neutrophils, macrophages, lymphocytes, and eosinophils were counted with an automatic erythrocyte analyzer (XT-2000iV, Sysmex Corporation, Hyogo, Japan).

2.7. Biochemical measurements

Lactate dehydrogenase (LDH) and total protein (TP) concentrations in the supernatant obtained by centrifugation of the BALF were measured with an automatic biochemical analyzer (TBA-200FR, Toshiba Medical Systems Corporation, Tochigi, Japan). Interleukin (IL)-1α, IL-1β, IL-2, IL-4, IL-6, IL-10, IL-12, granulocyte monocyte colony stimulating factor (GM-CSF), interferon (IFN)-γ, and tumor necrosis factor (TNF)-α concentrations were measured using a Rat Cytokine 10-Plex A Panel kit and Bio-Plex Suspension Array System (Bio-Rad Laboratories, Inc., Tokyo, Japan).

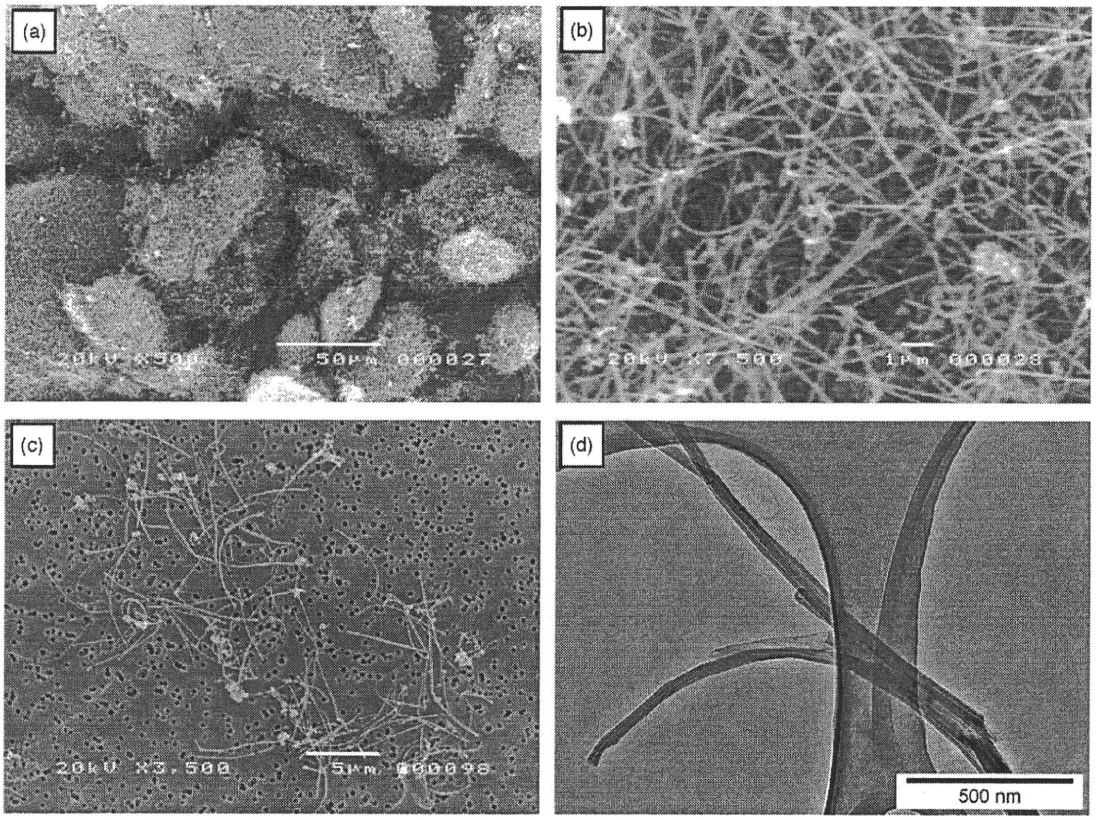

Fig. 1. SEM and TEM images of MWCNTs samples. SEM images of bulk MWCNTs (panels a and b). SEM (panel c) and TEM (panel d) images of MWCNTs dispersed by ultrasonication with an ultrasonic bath.

2.8. Histopathological evaluation

The trachea, left lung, liver, kidney, spleen, and cerebrum were fixed with 10% (v/v) neutral phosphate-buffered formalin solution, embedded in paraffin, sectioned, and stained with hematoxylin and eosin for histopathological evaluation under the light microscope.

2.9. Light and electron microscopic observation of MWCNTs in the lung

Morphology of the MWCNTs in the lung was observed with the light microscope. Sections of the right lung after lavage were fixed with glutaraldehyde and were resin-embedded to give ultrathin sections. Morphology of the individual tubes of instilled MWCNTs in the lung of rats was observed with TEM (JEM-100CX II, JEOL Ltd., Tokyo, Japan).

2.10. Statistical analyses

Statistical analyses of the body and lung weights, as well as the cell numbers and biochemical parameters in the BALF were conducted. Statistical significance was determined using multiple comparison tests between the negative control and MWCNT-exposed groups. First, the Bartlett's test was conducted. One-way layout analysis of variance was conducted when the variances were equal. Further, Dunnett's multiple comparison tests were conducted when the differences between the groups were significant. The Kruskal–Wallis test was used when the variances were not equal and Steel's multiple comparison tests were conducted when the differences were significant. Statistical significance was determined between the positive and negative control groups using intergroup comparison tests. First, the *F*-test was conducted; the Student's *t*-test was used when the variances were equal, and the Aspin–Welch *t*-test was used when the variances were not equal. Statistical significances were judged at the 0.05 probability level. SAS System version 6.12 (SAS Institute Japan Ltd., Tokyo, Japan) was used for all the statistical analyses.

3. Results

3.1. MWCNT characterization

SEM and TEM images of the bulk and dispersed MWCNT samples are shown in Fig. 1. In the bulk MWCNT samples, MWCNTs were in the form of agglomerates with sizes ranging from 50 to 100 μm, which are formed from tangled individual tubes with lengths of more than 10 μm (Fig. 1a). Objects other than fibrous shape materials (sizes less than 1 μm), which were considered to be carbon soot, were also observed in the bulk MWCNT samples (Fig. 1b). Their content was 7–8% by weight and catalysts were not detected (<0.1% by weight), based on results from the TG analysis. The BET surface area of the bulk MWCNTs was 23.0 m^2/g.

Most of the MWCNTs in the suspension were individually dispersed (Fig. 1c and d), which suggests that ultrasonication with an ultrasonic bath is effective for dispersing MWCNTs into the Tween 80 solution. Distribution of the MWCNT length in the 1 mg/mL of MWNT suspension, which is measured based on the SEM images, is shown in Fig. 2. The length of the all MWC-

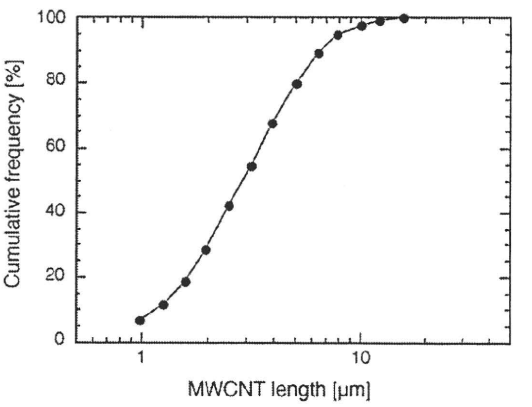

Fig. 2. Distribution of MWCNT length in a 1 mg/mL MWCNT suspension dispersed by ultrasonication in an ultrasonic bath.

NTs in the suspension was less than 20 μm, whereas longer tubes were present in the bulk sample. These results suggest that the MWCNTs were cut during ultrasonication. Generally ultrasonication processes can cause a degradation in sample quality by introducing defects in the graphene structure of MWCNT and producing carbon debris. In order to evaluate this degradation, an effective method is calculation of D/G ratio, the ratio of the intensities of disorder-induced mode (D-band) and graphene-induced mode (G-band) which are appeared in the Raman spectrum of MWCNT (Lee et al., 2008; Musumeci et al., 2008). The D/G ratio of the bulk MWCNT samples and the dispersed MWCNT suspension showed quite similar values of 0.091 and 0.085, respectively. This result implies that there are not significant degradation in sample quality after the ultrasonication process even the MWCNT fibers were cut into shorter segments.

3.2. Body and lung weights

Statistically significant differences in the body weights of experimental animals were not observed between any of the MWCNT or crystalline silica-exposed groups and the negative control group at any time point.

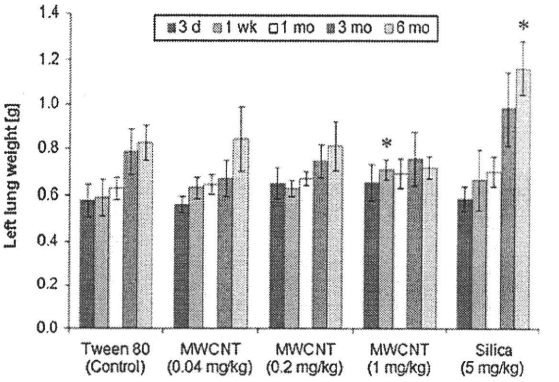

Fig. 3. Left lung weights of rats exposed to MWCNTs or crystalline silica particles and the corresponding controls at 3-day, 1-week, 1-month, 3-month, and 6-month post-instillation exposure. Values are represented as the mean ± SD. *Significant increase from control ($p < 0.05$).

Throughout the study period, no obvious increase in the lung weight was observed in any of the MWCNT-exposed groups when compared with the lung weight in the negative control group. In contrast, lung weight was significantly greater in the crystalline silica-exposed group (Fig. 3).

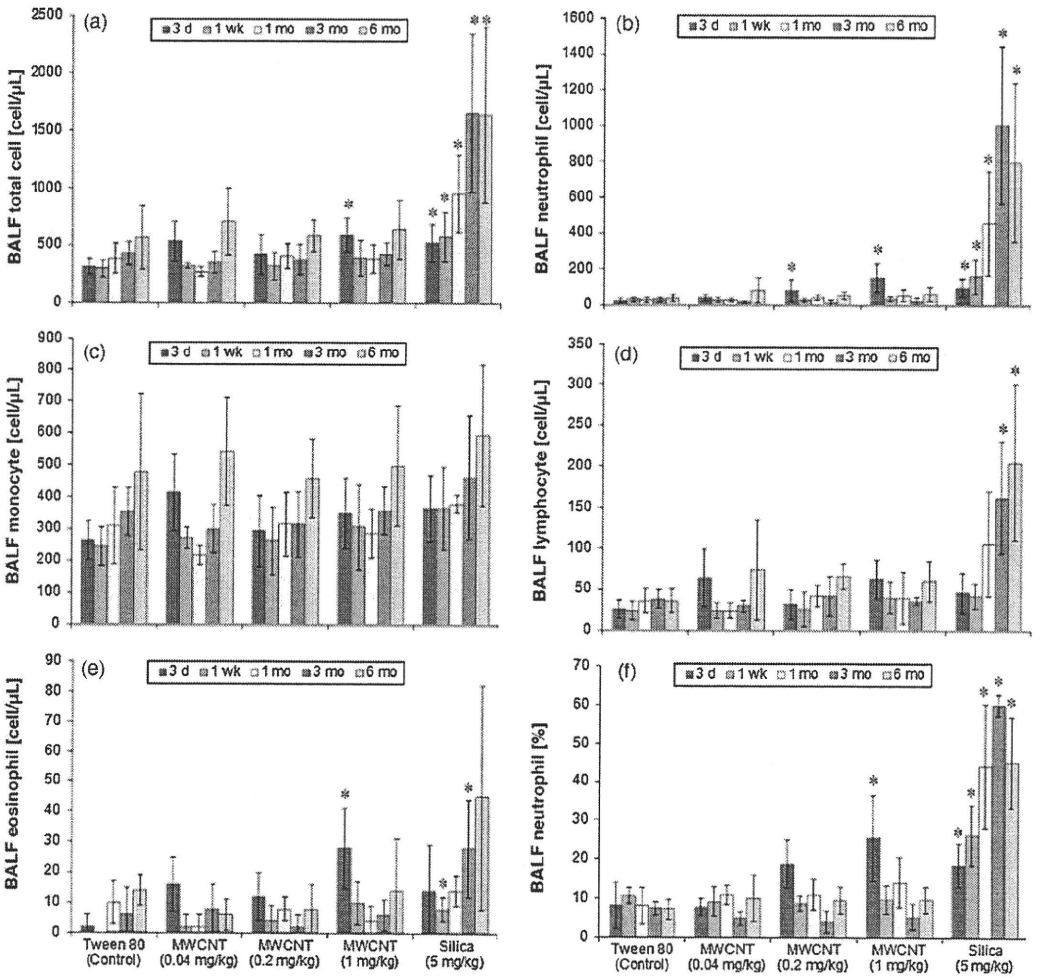

Fig. 4. Total number of BALF cells (a), neutrophils (b), macrophages (c), lymphocytes (d), and eosinophils (e), and the percentage of neutrophils (f) in rats exposed to MWCNTs, crystalline silica particles, or the corresponding controls at 3-day, 1-week, 1-month, 3-month, and 6-month post-instillation exposure. Values are represented as the mean ± SD. *Significant increase from control ($p < 0.05$).

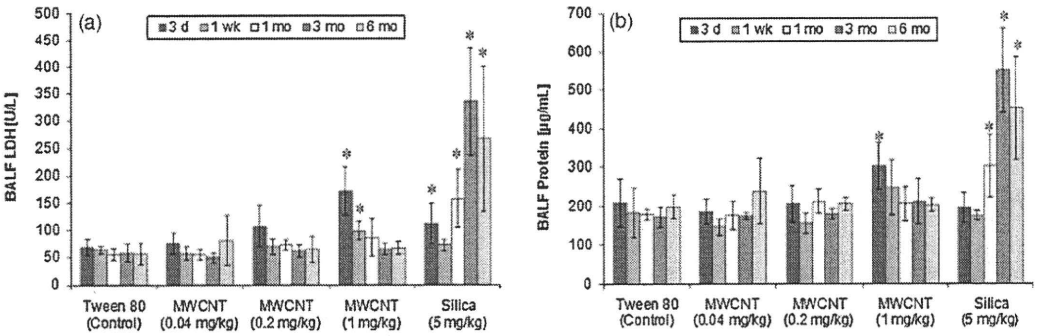

Fig. 5. BALF LDH (a) and protein (b) levels in rats exposed to MWCNTs, crystalline silica particles, or the corresponding controls at 3-day, 1-week, 1-month, 3-month, and 6-month post-instillation exposure. Values are represented as the mean ± SD. *Significant increase from control ($p < 0.05$).

3.3. Necropsy findings

In the negative control group and the group exposed to 0.04 mg/kg MWCNTs, abnormal findings were not observed at any of the time points. In the groups exposed to 0.2 and 1 mg/kg MWCNTs, brown or black spots were observed in the lung until 1- and 6-month post-exposure, respectively. These spots were considered to be the pigment of the agglomerated MWCNTs. In the crystalline silica-exposed group, significant changes were not observed until 1-month post-exposure, white spots were observed in the lung from 3- to 6-month post-exposure, and hypertrophy of the peribronchial lymph nodes and thymic lymph nodes was observed.

3.4. BALF results

3.4.1. Inflammatory cells

In the MWCNT-exposed groups, the number and percentage of BALF inflammatory cells were changed in a dose-dependent manner (Fig. 4). While no changes were observed in the group exposed to 0.04 mg/kg MWCNTs. BALF neutrophils were increased significantly only at 3-day post-exposure in the group exposed to 0.2 mg/kg MWCNTs. In the group exposed to 1.0 mg/kg MWCNTs, the total BALD cell numbers, neutrophils, eosinophils, and the percentage of neutrophils were increased significantly only at 3-day post-exposure. In the crystalline silica-exposed group, the total BALF cell numbers, neutrophils, lymphocytes, eosinophils, and

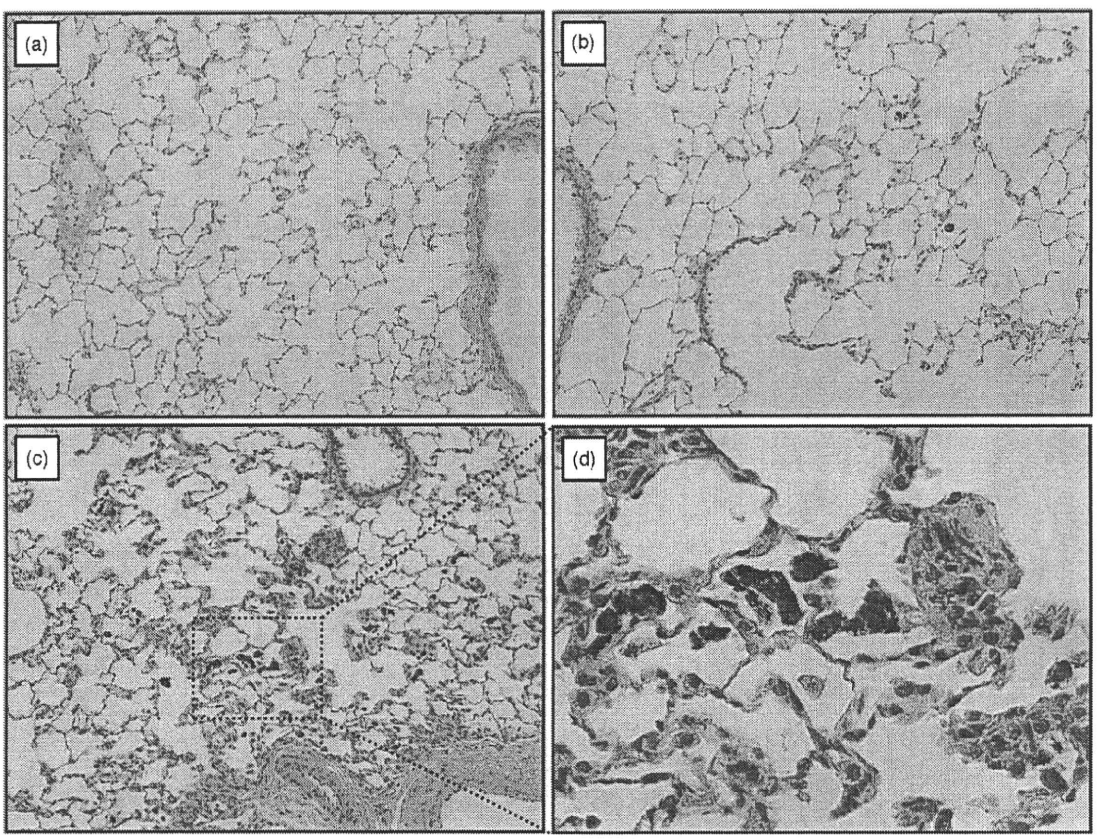

Fig. 6. Light micrographs of lung tissues of rats exposed to MWCNTs at 1-month post-instillation exposure (hematoxylin and eosin staining). No significant changes were observed in the group exposed to 0.04 mg/kg MWCNTs (panel a). Minimal macrophage accumulation and phagocytosed MWCNTs were observed in the alveoli of the group exposed to 0.2 mg/kg MWCNTs (panel b). MWCNT deposits and macrophage accumulation were observed in the alveoli of the group exposed to 1 mg/kg MWCNTs (panels c and d).

Table 1
Pulmonary histopathology severity scores[a] of rats exposed to MWCNTs or silica.

Findings	Timepoint	Control group	MWCNT-exposed group			Silica-exposed group
			0.04 mg/kg	0.2 mg/kg	1 mg/kg	
Administered substance accumulation in the alveoli	3 d	0	0	1	1	1
	1 wk	0	0	1	1.4	0.8
	1 mo	0	0	0.6	1	1
	3 mo	0	0	0.4	1	0
	6 mo	0	0	0.6	1	0
Administered substance accumulation in the interstitium	3 d	0	0	0	0.6	1
	1 wk	0	0	0	0.8	0
	1 mo	0	0	0.2	0.4	0
	3 mo	0	0	0.2	0.4	0
	6 mo	0	0	0	1.2	0
Inflammatory cell infiltration in the alveoli	3 d	0.2	0.2	0.8	0.8	0.6
	1 wk	0	0	0.4	0.4	0
	1 mo	0.4	0	0	0	0.2
	3 mo	0	0	0	0	0.6
	6 mo	0	0	0	0	1
Macrophage accumulation in the alveoli	3 d	0.6	0.2	1	1.4	1
	1 wk	0.2	0	1	1.4	0.8
	1 mo	0.2	0	0.8	1	1
	3 mo	0	0	0.4	1	1.8
	6 mo	0	0	0.6	1	2
Macrophage infiltration in the interstitium	3 d	0.4	0	0.6	1.2	1
	1 wk	0.2	0	0.2	1.2	0
	1 mo	0	0	0.2	0.4	0.6
	3 mo	0	0	0.2	0.4	1
	6 mo	0	0	0	1.2	0.3
Granuloma in the interstitium	3 d	0.4	0	0.6	0.4	0.2
	1 wk	0	0	0	0.4	0
	1 mo	0	0	0.2	0.4	0
	3 mo	0	0	0	0	0.2
	6 mo	0	0	0	0.4	0.8
Granuloma in the lymphoid tissue	3 d	0	0	0	0	0
	1 wk	0	0	0	0	0
	1 mo	0	0	0	0	0
	3 mo	0	0	0	0	0
	6 mo	0	0	0	0	1
Hypertrophy of the bronchial epithelium	3 d	0	0	1.4	1	0
	1 wk	0	0	0	0.2	0
	1 mo	0	0	0	0	0
	3 mo	0	0	0	0	0
	6 mo	0	0	0	0	0
Hypertrophy of the alveolar epithelium	3 d	0	0	0	0	0
	1 wk	0	0	0	0	0
	1 mo	0	0	0	0	0
	3 mo	0	0	0	0	0.8
	6 mo	0	0	0	0	1.8
Macrophage cytolysis in the alveoli	3 d	0	0	0	0	0
	1 wk	0	0	0	0	0
	1 mo	0	0	0	0	0.2
	3 mo	0	0	0	0	1.8
	6 mo	0	0	0	0	1.8
Foamy macrophage infiltration in the alveoli	3 d	0	0	0	0	0
	1 wk	0	0	0	0	0
	1 mo	0	0	0	0	0
	3 mo	0	0	0	0	1.4
	6 mo	0	0	0	0	1.3
Alveolar proteinosis	3 d	0	0	0	0	0
	1 wk	0	0	0	0	0
	1 mo	0	0	0	0	0
	3 mo	0	0	0	0	1.2
	6 mo	0	0	0	0	1.8

[a] Severity scores given to individual animals from a complete pathological examination are 0, not remarkable; 1, minimal; 2, slight/mild; 3, moderate; and 4, severe; based upon relative evaluation of lesions. Severity scores for each animal within a group were added, and an average score per animal was calculated, which is shown in the table.

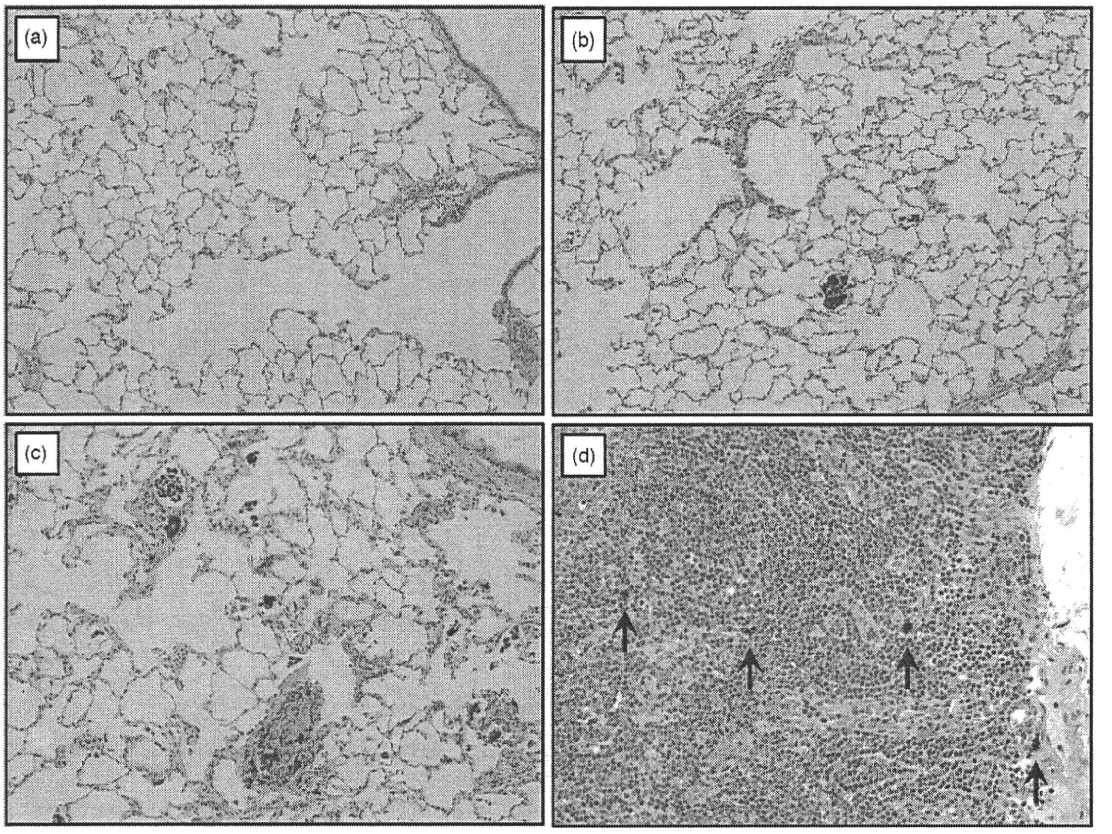

Fig. 7. Light micrographs of lung tissues of rats exposed to MWCNTs at 6-month post-instillation exposure (hematoxylin and eosin staining). No significant changes were observed in the group exposed to 0.04 mg/kg MWCNTs (panel a). Minimal macrophage accumulation and phagocytosed MWCNTs were observed in the alveoli of the group exposed to 0.2 mg/kg MWCNTs (panel b). MWCNT deposits and macrophage accumulation were observed in the alveoli and interstitium of the group exposed to 1 mg/kg MWCNTs (panel c). Minimal MWCNT depositions (arrows) were observed in the peribronchial lymph nodes in the group exposed to 1 mg/kg MWCNTs (panel d).

the percentage of neutrophils were significantly increased until 6-month post-exposure.

3.4.2. Biochemical measurements

For the MWCNT-exposed groups, LDH and TP levels in the BALF were significantly increased only in the group exposed to 1 mg/kg MWCNTs; however, the changes were transient and recovered after 1-week post-exposure (Fig. 5). BALF cytokine levels were not significantly changed at any time point (data not shown). In contrast, LDH and TP levels in the BALF were significantly increased until 6-month post-exposure in the crystalline silica-exposed group (Fig. 5), and significant changes in IL-1β and IL-2 levels were observed in this group (data not shown).

3.5. Histopathological evaluation

For all the groups, histopathological changes due to the instillation exposure of MWCNTs or crystalline silica were observed only in the lungs and lung-associated lymph nodes, and not in the other tissues (i.e., the liver, kidney, spleen, and cerebrum). Table 1 summarizes the histopathological findings of the rats examined in this study and their severity scores at each time point.

In the MWCNT-exposed groups, dose-dependent histopathological changes were observed. In the group exposed to 0.04 mg/kg MWCNTs, no significant changes were observed at any time points (Figs. 6 and 7Figs. 6a and 7a). In the group exposed to 0.2 mg/kg MWCNTs, minimal macrophage accumulation and phagocytosed MWCNTs were observed in the alveoli (Figs. 6b and 7b). In the group exposed to 1 mg/kg MWCNTs, deposition of the MWCNTs and macrophage accumulation, part of which were granulomatous, was observed in the alveoli and interstitium from 3-day to 1-month post-exposure (Fig. 6c and d). Most MWCNTs were phagocytosed by alveolar macrophages. Further, hypertrophy of the bronchial epithelium and inflammatory cell infiltrations were observed. From 3- to 6-month post-exposure, histopathological findings were qualitatively similar to those at 1-month post-exposure; although the severity of the changes was gradually weaker. At 6-month post-exposure, deposition of the MWCNTs and macrophage accumulation, part of which were granulomatous, was observed in the alveoli and interstitium in the group exposed to 1 mg/kg MWCNTs; however, the severity of these changes was minimal (Fig. 7c). In the group exposed to 1 mg/kg MWCNTs, minimal MWCNT depositions were observed in the peribronchial lymph nodes at 6-month post-exposure (Fig. 7d).

In the crystalline silica-exposed group, only minimal macrophage accumulation in the alveoli and interstitium was observed up to 1-week post-exposure. However, the severity of macrophage accumulation was increased after 1-month post-exposure, and, cytolysis of macrophages was observed, which was most severe at 6-month post-exposure. At 6-month post-exposure, in addition to the infiltration of inflammatory cells, foamy macrophages and cytolysis of macrophages were observed in the alveoli; pulmonary alveolar proteinosis was induced (Fig. 8a). Hypertrophy of the alveolar epithelium and granulomas was observed in the interstitium (Fig. 8b). Multifocal granulomas were also observed in the intrapulmonary lymph nodes (Fig. 8c), peribronchial lymph nodes (Fig. 8d), and thymic lymph nodes (data not shown).

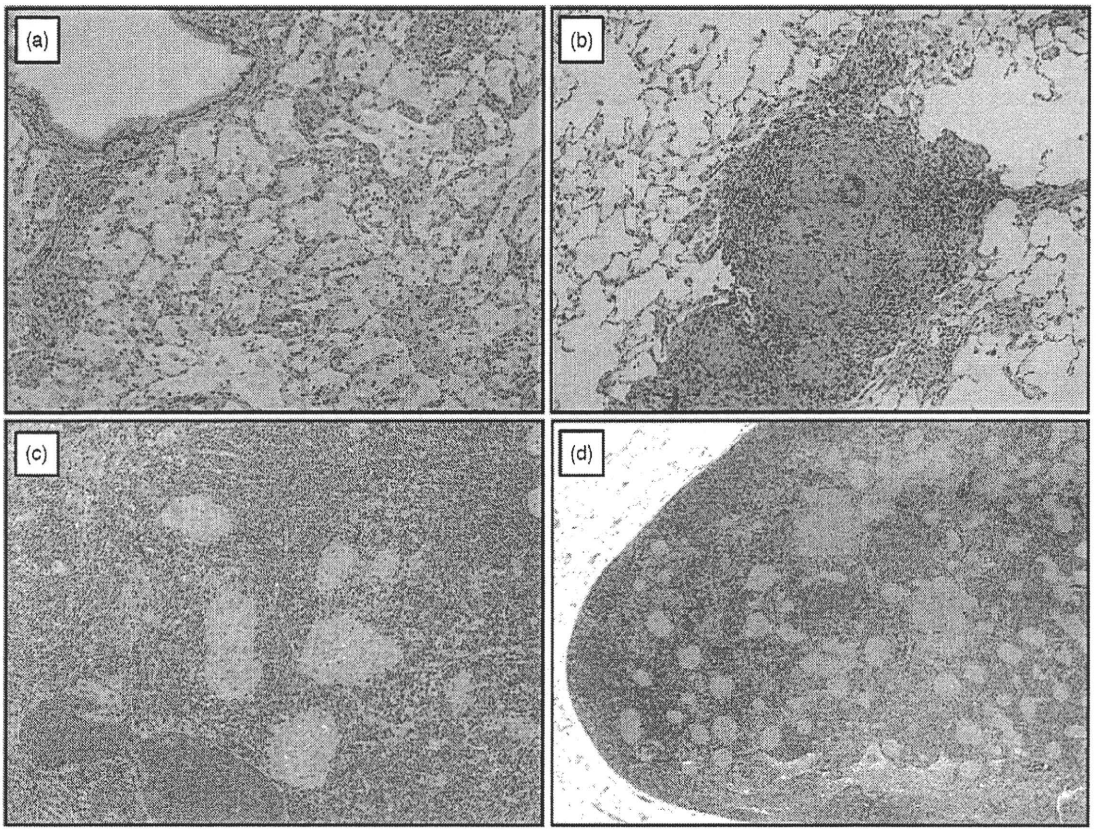

Fig. 8. Light micrographs of lung tissues of rats exposed to crystalline silica particles at 6-month post-instillation exposure (hematoxylin and eosin staining). Cytolysis of macrophages and foamy macrophage infiltrations were observed in the alveoli; pulmonary alveolar proteinosis was induced (panel a). Granuloma formations were observed in the interstitium (panel b). Multifocal granulomas were observed in the intrapulmonary lymph nodes (panel c) and peribronchial lymph nodes (panel d).

The results of the histopathological evaluations were consistent with that of BALF inflammatory cells and biochemical measurements.

3.6. Light and electron microscopic observation of MWCNTs in the lungs

On the basis of light microscopic examination, MWCNTs deposited in the lungs were phagocytosed by alveolar macrophages and were sequentially accumulated in the alveoli or interstitium until 6-month post-exposure (Fig. 9). Furthermore, the 400 TEM images, which displayed individual MWCNTs, showed that all the MWCNTs were presented in a similar form in the lungs. MWCNTs were located in the alveolar macrophages or in macrophages in the interstitial tissues, and individual MWCNTs were not present in the cells of the interstitial tissue (Fig. 10). The diameter and length of the 104 tubes in the TEM images were measured. The diameter of the MWCNTs in the lungs was almost the same as the instilled materials (approximately 60 nm). There were a wide range of MWCNT lengths in the lungs; the median length was approximately 1.5 μm (number basis), although some tubes were considerably longer, measuring up to 6 μm (Fig. 11).

4. Discussion

Biological responses due to the single instillation of MWCNTs were observed only in the lungs of rats, and not in the liver, kidney, spleen, or cerebrum (including the olfactory bulb) in all the groups. BALF inflammatory cells as well as LDH and TP levels were significantly increased in the group exposed to 1 mg/kg MWCNTs, but only at 3-day post-exposure. No significant changes in BALF inflammatory cells and markers were observed in the groups exposed to 0.04 and 0.2 mg/kg MWCNT at any time points. The severity of the lesions on histopathological examination of rat lungs was dose dependent although Warheit et al. (2004) and Mitchell et al. (2007) have reported non-dose-dependent pulmonary responses due to instillation of SWCNTs or inhalation of MWCNTs. Histopathological evaluation indicated deposition of the MWCNTs and macrophage infiltration, part of which were granulomatous, in the alveoli and interstitium in the group exposed to 1 mg/kg MWCNTs. On the basis of the light microscopic observations, MWCNTs were phagocytosed by macrophages. Hypertrophy of the bronchial epithelium and inflammatory cell infiltrations were also observed in this group. Some of the previous toxicity studies of MWCNT instillation or inhalation exposures in rats (Muller et al., 2005; Li et al., 2007; Ma-Hock et al., 2009; Pauluhn, 2010) have reported qualitatively similar pulmonary responses. However, our study revealed that pulmonary inflammatory responses were transient, and the histopathological changes were gradually weaker from 1-week to 6-month post-exposure. At 6-month post-exposure, significant changes were not observed in the group exposed to 0.2 mg/kg MWCNTs. In the group exposed to 1 mg/kg MWCNTs, deposition of the MWCNTs and macrophage accumulation, of which some of them were granulomatous, were observed in the alveoli and interstitium until 6-month post-exposure, although they were minimal changes. Studies have reported that pulmonary fibrosis is induced due to exposure to SWCNTs or MWCNTs (Muller et al., 2005; Shvedova et al., 2008a); however, pulmonary fibrosis was not observed in any of the groups in this study.

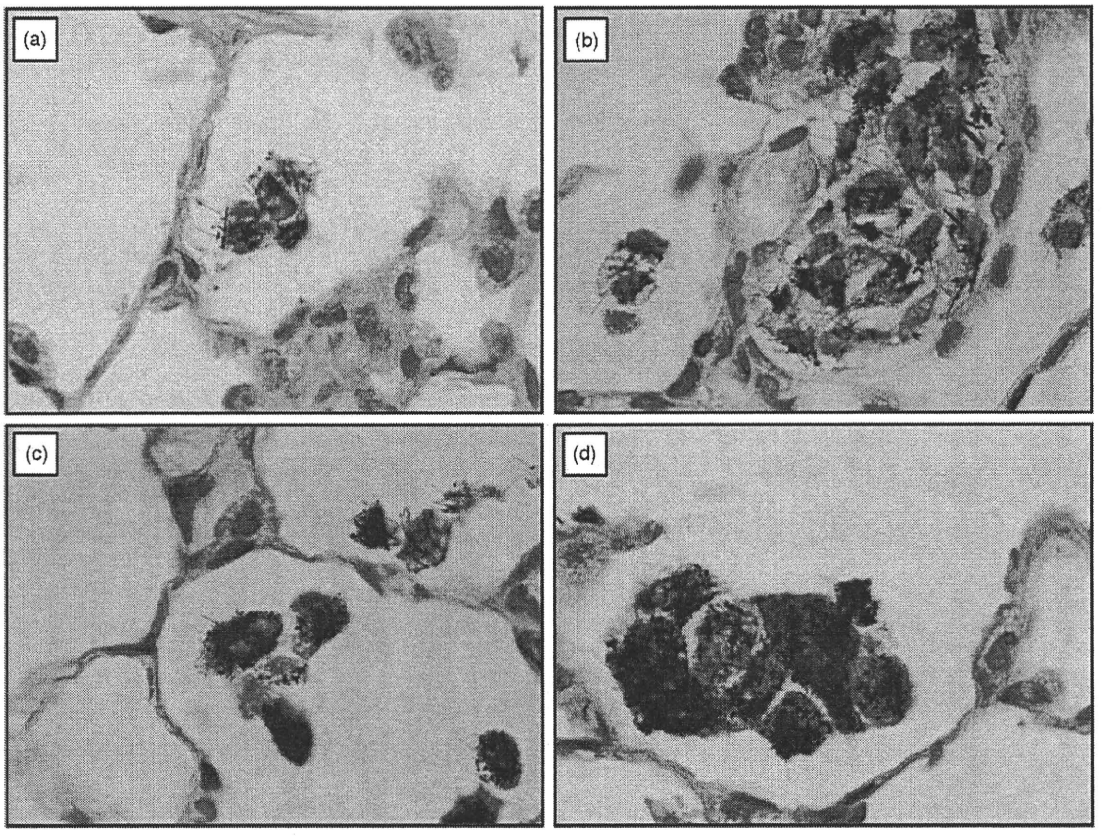

Fig. 9. Light micrographs of MWCNTs in the lungs of rats exposed to 1 mg/kg MWCNTs at 3-day (panel a), 1-week (panel b), 1-month (panel c), and 6-month (panel d) post-instillation exposure (hematoxylin and eosin staining, magnification: ×200). MWCNTs deposited in the lungs were typically phagocytosed by alveolar macrophages and were sequentially accumulated in the alveoli until 6-month post-instillation.

Light microscopy and TEM observations revealed that the MWCNTs deposited in the lungs were phagocytosed by alveolar macrophages and were sequentially accumulated in the alveoli. MWCNT translocation or penetration to the pleural was not observed. Furthermore, based on the 400 TEM images, it was shown that all the MWCNTs were located in the alveolar macrophages or phagocytosed by macrophages in the interstitial tissues, and individual MWCNTs were not presented in the cells of the interstitial tissue.

In contrast, inflammatory responses were observed in the lungs and lung-associated lymph nodes in the group exposed to 5 mg/kg crystalline silica, where BALF inflammatory cells, LDH, TP, IL-1β, and IL-2 levels were significantly increased after the instillation exposure, and these changes were the most severe at 6-month post-exposure. Furthermore, lung weights were significantly increased at 3- and 6-month post-exposure. Histopathological evaluation revealed that although short-term inflammatory responses were weak, the inflammatory responses were much stronger at 6-month post-exposure. Consequently, crystalline silica particles produced continuous inflammation with a 5 mg/kg dose of intratracheal instillation. These pulmonary responses were qualitatively and quantitatively different from the responses observed for MWCNTs instillation exposure.

The relationship of the dose of MWCNTs instilled into the lungs in this study and exposure levels of aerosolized MWCNTs to humans during the handling of CNTs in the work place is discussed below. The pulmonary deposition amount of MWCNTs in this study was considered to be almost 100% of the instilled dose of the MWCNTs (i.e., 0.04, 0.2, and 1.0 mg/kg). By measuring the BET surface area of the MWCNT samples, the doses can be expressed in terms of the CNT surface area dose, which are 0.0009, 0.1146, and 0.023 m^2/kg, for doses of 0.04, 0.2, and 1.0 mg/kg, respectively. Based on the density of the MWCNT samples reported by the manufacturer (2.1 g/cm^3) and assuming that the tube diameter and length are uniform (60 nm and 1.5 μm, respectively), and that all tubes are individually dispersed in the suspension, the doses can also be expressed in terms of tube numbers, which are 9.4×10^9, 4.7×10^{10}, and 2.4×10^{11} tubes/kg, for dosed of 0.04, 0.2, and 1.0 mg/kg, respectively.

On the other hand, there are only a few reports of atmospheric CNT concentrations measurements in the work place. Maynard et al. (2004) and Han et al. (2008) reported measured concentrations of SWCNTs and MWCNTs in the research facilities, respectively.

Maynard et al. (2004) reported that atmospheric concentrations of SWCNTs, which were estimated using an indicator of metal catalysts, were in range of 0.7–53 $\mu g/m^3$ during the collection and cleaning process, based on the investigation of SWCNT research facilities with laser-abrasion or the high pressure carbon monoxide (HiPco) method. Han et al. (2008) reported that the atmospheric mass concentration of total dust (including MWCNTs) was in range of 210–430 $\mu g/m^3$ during the blending process and in range of 37–190 $\mu g/m^3$ during the weighing and spraying process, based on the investigation of MWCNT research facilities with the thermal chemical vapor deposition (CVD) method. They also reported that the number concentration of MWCNTs was in range of 172.9–193.6 $\times 10^6$ tubes/m^3 during these processes. Based on the atmospheric mass concentration or number concentration of CNTs reported in these studies, deposition amounts of MWCNTs to the lungs of humans working for 8 h/day and 5 days/week without any exposure protection can be calculated as

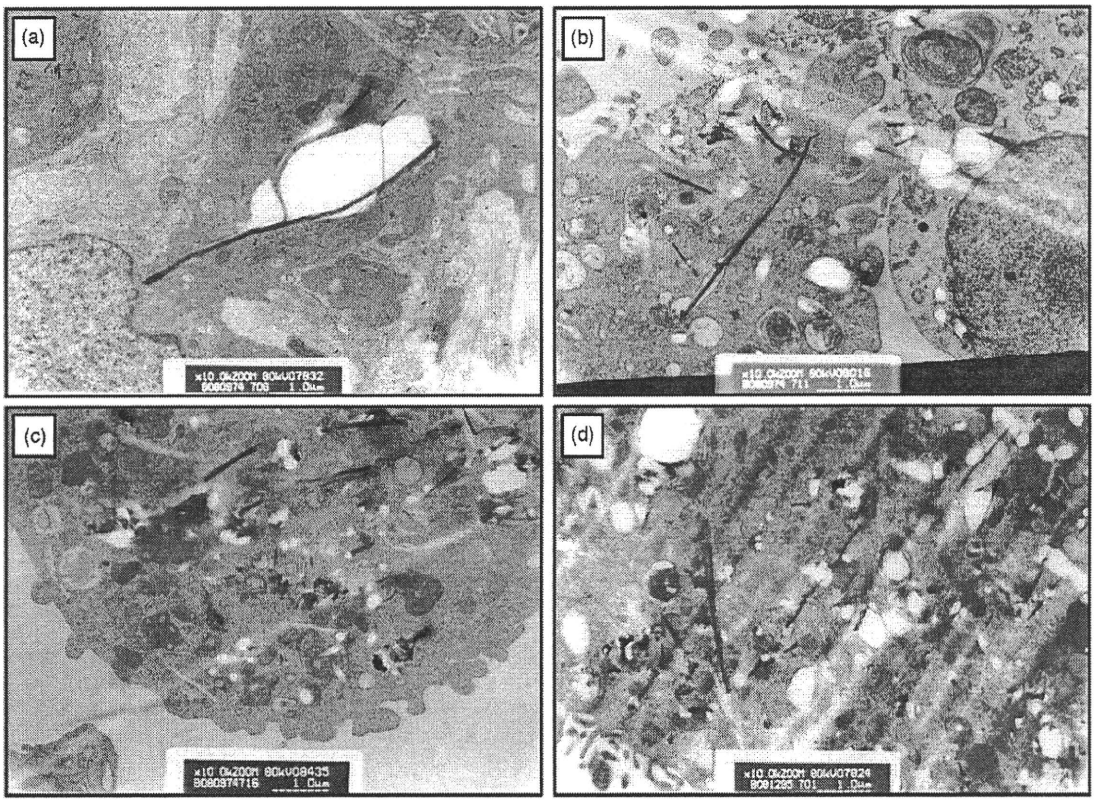

Fig. 10. TEM images of the lungs of rats exposed to 1 mg/kg of MWCNTs at 1-week (panel a), 1-month (panel b), 3-month (panel c), and 6-month (panel d) post-instillation exposure (magnification: ×10,000). MWCNTs observed in TEM images were located in the alveolar macrophages and not in the interstitial cells.

follows. Assuming that average daily exposure time is 8 h/day × 5 days/week × 60 min/h = 343 min/day, the deposition fraction of inhaled MWCNTs into the lungs is 0.1 (10%) based on the study of Miller (2000), the respiratory minute volume is 25 L/min, and body weight is 60 kg, then pulmonary deposition amounts of MWCNTs are calculated to be 0.01 and 6.2 μg/kg/day, based on the atmospheric concentration of 0.7 μg/m^3 (Maynard et al., 2004) and 434.5 μg/m^3 (Han et al., 2008), respectively. Therefore, instillation exposure of 1.0 mg/kg MWCNTs corresponds to pulmonary deposition amounts of 160–1300 days (i.e., several months to several years) in the working environment without any exposure protection when the maximum atmospheric concentration of MWCNTs is used in the calculation.

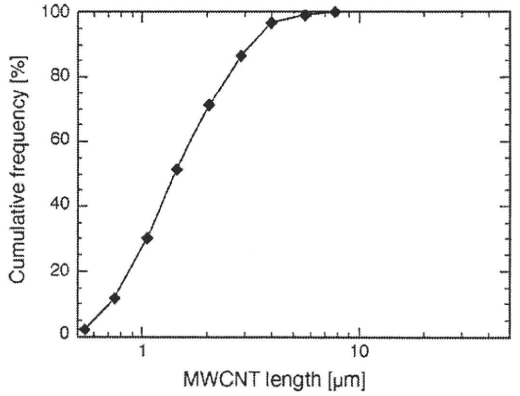

Fig. 11. Length of MWCNTs in the lungs of rats exposed to 1 mg/kg MWCNTs. The lengths of 104 MWCNTs observed by the TEM were measured. The median (minimum–maximum) length of the MWCNTs in the lungs was 1.5 (0.42–6.1) μm.

Based on the number concentration of CNTs, deposition of MWCNTs into the lungs per day per kg body weight were calculated to be 2.47–2.77 × 10^6 tubes/kg/day based on the atmospheric number concentration of 172.9–193.6 × 10^6 tubes/m^3 (Han et al., 2008). Therefore, 2.4 × 10^{11} tubes/kg (1.0 mg/kg) of instillation exposure of MWCNTs corresponds to a pulmonary deposition amount of 85,000–95,000 days, which is longer than the average human lifespan.

Collectively, our data indicated that the pulmonary inflammatory responses to MWCNT deposition in the lungs were dose dependent, and the responses were weak and transient under approximate pulmonary deposition amounts comparable to the work environment. Chronic inflammatory responses such as pulmonary fibrosis or angiogenesis were not observed. MWCNTs deposited in the lungs were mostly phagocytosed by alveolar macrophages and were sequentially accumulated in the alveoli, which suggests that MWCNTs were being processed and cleared by alveolar macrophages.

Competing interests

The authors declare that they have no competing interests.

Acknowledgments

The authors wish to thank Dr. Michihito Takahashi for contributing to the histopathological evaluation conducted in this study. This study was conducted under the "Evaluating Risks Associated with Manufactured Nanomaterials" Project (P06041) funded by the New Energy and Industrial Technology Development Organization (NEDO), Japan.

References

Chou, C.C., Hsiao, H.Y., Hong, Q.S., Chen, C.H., Peng, Y.W., Chen, H.W., Yang, P.C., 2008. Single-walled carbon nanotubes can induce pulmonary injury in mouse model. Nano Lett. 8, 437–445.

Han, J.H., Lee, E.J., Lee, J.H., So, K.P., Lee, Y.H., Bae, G.N., Lee, S.B., Ji, J.H., Cho, M.H., Yu, I.J., 2008. Monitoring multiwalled carbon nanotube exposure in carbon nanotube research facility. Inhal. Toxicol. 20, 741–749.

Kobayashi, N., Naya, M., Endoh, S., Maru, J., Yamamoto, K., Nakanishi, J., 2009. Comparative pulmonary toxicity study of nano-TiO_2 particles of different sizes and agglomerations in rats: different short- and long-term post-instillation results. Toxicology 264, 110–118.

Lam, C.W., James, J.T., McCluskey, R., Hunter, R.L., 2004. Pulmonary toxicity of single-wall carbon nanotubes in mice 7 and 90 days after intratracheal instillation. Toxicol. Sci. 77, 126–134.

Lee, S., Peng, Jr-W., Liu, C.-H., 2008. Raman study of carbon nanotube purification using atmospheric pressure plasma. Carbon 46, 2124–2132.

Li, J.G., Li, W.X., Xu, J.Y., Cai, X.Q., Liu, R.L., Li, Y.J., Zhao, Q.F., Li, Q.N., 2007. Comparative study of pathological lesions induced by multiwalled carbon nanotubes in lungs of mice by intratracheal instillation and inhalation. Environ. Toxicol. 22, 415–421.

Ma-Hock, L., Treumann, S., Strauss, V., Brill, S., Luizi, F., Mertler, M., Wiench, K., Gamer, A.O., van Ravenzwaay, B., Landsiedel, R., 2009. Inhalation toxicity of multi-wall carbon nanotubes in rats exposed for 3 months. Toxicol. Sci. 112, 468–481.

Mangum, J.B., Turpin, E.A., Antao-Menzes, A., Cesta, M.F., Bermudez, E., Bonner, J.C., 2006. Single-walled carbon nanotube induced interstitial fibrosis in the lungs of rats is associated with increased levels of PDGF mRNA and the formation of unique intercellular carbon structures that bridge alveolar macrophages in situ. Part. Fibre Toxicol. 3, 15.

Maynard, A.D., Baron, P.A., Foley, M., Shvedova, A.A., Kisin, E.R., Castranova, V., 2004. Exposure to carbon nanotube material: aerosol release during the handling of unrefined singlewalled carbon nanotube material. J. Toxicol. Environ. Health. A 67, 87–107.

Mercer, R.R., Scabilloni, J., Wang, L., Kisin, E., Murray, A.R., Schwegler-Berry, D., Shvedova, A.A., Castranova, V., 2008. Alteration of deposition pattern and pulmonary response as a result of improved dispersion of aspirated single walled carbon nanotubes in a mouse model. Am. J. Physiol. Lung Cell. Mol. Physiol. 294, 87–97.

Miller, F.J., 2000. Dosimetry of particles in laboratory animals and humans in relationship to issues surrounding lung overload and human health risk assessment: a critical review. Inhal. Toxicol. 12, 19–57.

Mitchell, L.A., Gao, J., Wal, R.V., Gigliotti, A., Burchiel, S.W., McDonald, J.D., 2007. Pulmonary and systemic immune response to inhaled multiwalled carbon nanotubes. Toxicol. Sci. 100, 203–214.

Miyawaki, J., Yudasaka, M., Azami, T., Kubo, Y., Iijima, S., 2008. Toxicity of single-walled carbon nanohorns. ACS Nano 2, 213–226.

Muller, J., Huaux, F., Moreau, N., Misson, P., Heilier, J.F., Delos, M., Arras, M., Fonseca, A., Nagy, J.B., Lison, D., 2005. Respiratory toxicity of multi-wall carbon nanotubes. Toxicol. Appl. Pharmacol. 207, 221–231.

Muller, J., Delos, M., Panin, N., Rabolli, V., Huaux, F., Lison, D., 2009. Absence of carcinogenic response to multiwall carbon nanotubes in a 2-year bioassay in the peritoneal cavity of the rat. Toxicol. Sci. 110, 442–448.

Musumeci, A.W., Waclawik, E.R., Frost, R.L., 2008. A comparative study of single-walled carbon nanotube purification techniques using Raman spectroscopy. Spectrochim. Acta Part A 71, 140–142.

Pauluhn, J., 2010. Subchronic 13-week inhalation exposure of rats to multiwalled carbon nanotubes: toxic effects are determined by density of agglomerate structures, not fibrillar structures. Toxicol. Sci. 113, 226–242.

Poland, G.A., Duffin, R., Kinloch, I., Maynard, A., Wallace, W.A.H., Seaton, A., Stone, V., Brown, S., MacNee, W., Donaldson, K., 2008. Carbon nanotubes introduced into the abdominal cavity ofmice show asbestoslike pathogenicity in a pilot study. Nat. Nanotechnol. 3, 423–428.

Porter, D.W., Hubbs, A.F., Mercer, R.R., Wu, N., Wolfarth, M.G., Sriram, K., Leonard, S., Battelli, L., Schwegler-Berry, D., Friend, S., Andrew, M., Chen, B.T., Tsuruoka, S., Endo, M., Castranova, V., 2010. Mouse pulmonary dose- and time course-responses induced by exposure to multi-walled carbon nanotubes. Toxicology 269, 136–147.

Shvedova, A.A., Kisin, E.R., Mercer, R., Murray, A.R., Johnson, V.J., Potapovich, A.I., Tyurina, Y.Y., Gorelik, O., Arepalli, S., Schwegler-Berry, D., Hubbs, A.F., Antonini, J., Evans, D.E., Ku, B.K., Ramsey, D., Maynard, A., Kagan, V.E., Castranova, V., Baron, P., 2005. Unusual inflammatory and fibrogenic pulmonary responses to single-walled carbon nanotubes in mice. Am. J. Physiol. Lung Cell. Mol. Physiol. 289, 698–708.

Shvedova, A.A., Kisin, E.R., Murray, A.R., Gorelik, O., Arepalli, S., Castranova, V., Young, S.H., Gao, F., Tyurina, Y., Oury, T.D., Kagan, V.E., 2007. Vitamin E deficiency enhances pulmonary inflammatory response and oxidative stress induced by single-walled carbon nanotubes in C57BL/6 mice. Toxicol. Appl. Pharmacol. 221, 339–348.

Shvedova, A.A., Kisin, E.R., Murray, A.R., Kommineni, C., Castranova, V., Fadeel, B., Kagan, V.E., 2008a. Increased accumulation of neutrophils and decreased fibrosis in the lung of NADPH oxidase-deficient C57BL/6 mice exposed to carbon nanotubes. Toxicol. Appl. Pharmacol. 231, 235–240.

Shvedova, A.A., Kisin, E., Murray, A.R., Johnson, V.J., Gorelik, O., Arepalli, O., Hubbs, A.F., Mercer, R.R., Keohavong, P., Sussman, N., Jin, J., Yin, J., Stone, S., Chen, B.T., Deye, G., Maynard, A., Castranova, V., Baron, P.A., Kagan, V.E., 2008b. Inhalation vs. aspiration of single-walled carbon nanotubes in C57BL/6 mice: inflammation, fibrosis, oxidative stress, and mutagenesis. Am. J. Physiol. Lung Cell. Mol. Physiol. 295, 552–565.

Takagi, A., Hirose, A., Nishimura, T., Fukumori, N., Ogata, A., Ohashi, N., Kitajima, S., Kanno, J., 2008. Induction of mesothelioma in p53+/− mouse by intraperitoneal application of multi-wall carbon nanotube. J. Toxicol. Sci. 33, 105–116.

Warheit, D.B., Laurence, B.R., Reed, K.L., Roach, D.H., Reynolds, G.A.M., Webb, T.R., 2004. Comparative pulmonary toxicity assessment of single-wall carbon nanotubes in rats. Toxicol. Sci. 77, 126–134.

Warheit, D.B., Webb, T.R., Sayes, C.M., Colvin, V.L., Reed, K.L., 2006. Pulmonary instillation studies with nanoscale TiO_2 rods and dots in rats: toxicity is not dependent upon particle size and surface area. Toxicol. Sci. 91, 227–236.

Warheit, D.B., Webb, T.R., Reed, K.L., Frerichs, S., Sayes, C.M., 2007a. Pulmonary toxicity study in rats with three forms of ultrafine-TiO_2 particles: differential responses related to surface properties. Toxicology 230, 90–104.

Warheit, D.B., Webb, T.R., Colvin, V.L., Reed, K.L., Sayes, C.M., 2007b. Pulmonary bioassay studies with nanoscale and fine quartz particles in rats: toxicity is not dependent upon particle size but on surface characteristics. Toxicol. Sci. 95, 270–280.

【特集】

OECD 化学物質対策の動向（第 16 報）

－第 27 回 OECD 高生産量化学物質初期評価会議（2008 年オタワ）

Progress on OECD Chemicals Programme (16) — SIAM 27 in Ottawa, 2008

高橋美加[1]、松本真理子[1]、宮地繁樹[2]、菅野誠一郎[3]、菅谷芳雄[4]、平田睦子[1]、小野敦[1]、
鎌田栄一[1]、江馬　眞[1*]、広瀬明彦[1]
1）国立医薬品食品衛生研究所安全性生物試験研究センター総合評価研究室、
2）（財）化学物質評価研究機構安全性評価技術研究所、3）（独）労働安全衛生総合研究所、
4）（独）国立環境研究所環境リスク研究センター、
*現：（独）産業技術総合研究所安全科学研究部門

Mika Takahashi[1], Mariko Matsumoto[1], Shigeki Miyachi[2], Seiichiro Kanno[3],
Yoshio Sugaya[4], Hirata-Koizumi Mutsuko[1], Ono Atsushi[1], Eiichi Kamata[1],
Makoto Ema[1*], and Akihiko Hirose[1]
1) Division of Risk Assessment, Biological Safety Research Center, National Institute of Health Sciences, 2) Chemicals Assessment and Research Center, Chemicals Evaluation and Research Institute, Japan, 3) National Institute of Occupational Safety and Health, and 4) Research Center for Environmental Risk, National Institute for Environmental Studies, and *present: Research Institute of Science for Safety and Sustainability, National Institute of Advanced Industrial Science and Technology

要旨：第 27 回 OECD 高生産量化学物質初期評価会議（SIAM 27）が 2008 年 10 月にオタワ（カナダ）で開催され、日本が担当した 3 物質（*p*-トルエンスルホン酸ナトリウム：CAS 番号 657-84-1、レゾルシノール：CAS 番号 108-46-3、N-シクロヘキシル-2-ベンゾチアゾールスルフェンアミド：CAS 番号 95-33-0）の初期評価プロファイル（SIAP）について合意が得られた。本稿では本会議で合意の得られたこれら 3 物質の初期評価文書について紹介する。
キーワード：OECD、HPV プログラム、SIDS 初期評価会議

Abstract: The 27th Screening Information Data Set (SIDS) Initial Assessment Meeting (SIAM 27) was held in Ottawa, hosted by Canada. The initial assessment documents of three substances, sodium *p*-toluenesulfonate (CAS number: 657-84-1), 1,3-benzenediol (CAS number: 108-46-3), and N-cyclohexyl-2-benzothiazolsulfenamide (CAS number: 95-33-0) were submitted by the Japanese Government with or without the collaboration with International Council of Chemical Associations (ICCA). These SIDS Initial Assessment Profiles (SIAPs) of the substances were agreed at the meetings. In this report, the documents of these substances are introduced.
Keywords: OECD, HPV programme, SIDS Initial Assessment Meeting

化学生物総合管理　第 6 巻第 2 号（2010.12）　180-188 頁
連絡先：〒158-8501 世田谷区上用賀 1-18-1　E-mail: hirose@nihs.go.jp
受付日：2010 年 1 月 25 日　　受理日：2010 年 6 月 27 日

1　はじめに

経済協力開発機構（Organisation for Economic Co-operation and Development：OECD）では、1992年に始まった高生産量化学物質点検プログラム（High Production Volume Chemical (HPV) Programme）により、加盟各国における高生産量化学物質の安全性の評価を行っている（長谷川ら 1999a、江馬 2006）。日本政府は初回より評価文書を提出しており、2001年からは国際化学工業協会協議会（International Council of Chemical Associations：ICCA）による評価文書の原案作成に伴い日本化学工業協会加盟企業も評価文書の原案作成に参加している。第26回までの初期評価会議（Screening Information Data Set (SIDS) Initial Assessment Meeting：SIAM）において日本政府が担当し結論および勧告が合意された化学物質の評価文書のヒト健康影響または環境影響・曝露情報部分については既に紹介してきた（長谷川ら 1999b、2000、2001；高橋ら 2004、2005a、2005b、2006a、2006b、2006c、2007a、2007b、2007c、2008、2009）。また、第1回SIAM（SIAM 1）からSIAM 18までの結果の概要およびSIAM 19からSIAM 27の各会議内容についても紹介してきた（松本ら 2005a、2005b、2006a、2006b、2007a、2007b、2007c、2008a、2008b、2009）。

本稿ではSIAM 27で合意に至った日本担当物質の評価文書の概要を紹介する。なお、OECDガイドラインに則した毒性試験についてはガイドライン番号を示したが、遺伝毒性に関しては1物質に対して多種の試験が行われることもあり、結果のみ簡潔に示すこととした。

2　SIAM 27で合意された日本担当物質の初期評価内容

2008年10月にオタワ（カナダ）で開催されたSIAM 27において、我が国は3物質の初期評価文書を提出し、それら全ての初期評価結果および勧告が合意された。

SIAMにおける合意はFW（The chemical is a candidate for further work.）またはLP（The chemical is currently of low priority for further work.）として示されている。FWは「今後も追加の調査研究作業が必要である」、LPは「現状の使用状況においては追加作業の必要はない」ことを示す。

（1）*p*-トルエンスルホン酸ナトリウム

英名 Sodium *p*-toluenesulfonate (657-84-1)（日本政府）

トルエン／キシレン／クメンの各スルホン酸塩（ナトリウム、アンモニウム、カルシウム、カリウム）の異性体（オルト、メタ、パラ）を含む、ヒドロトロープ類（Hydrotropes）カテゴリーに関する初期評価文書がSIAM 21（2005年）で承認されている。本物質は同カテゴリーに含まれるが、本物質に関する新たな試験データが得られたので、カテゴリーとは別に初期評価文書が作成された。

1）曝露状況

本物質は粉末の固結防止剤、洗剤の可溶化剤、染料の希釈剤として使用される。本物質は閉鎖系で製造・加工されるため、職業曝露の可能性は低い。また、本物質の製造・加工過程における廃水から環境中への排出量に関しては、現在利用可能な測定データはないが、廃水処理が行われているので少ないと考えられる。本物質は製品に含まれるため、皮膚接触での消費者曝露の可能性があり、また、事故による曝露も考えられるが、容易に洗浄可能なので、その摂取量は軽減されると考えられた。

2）環境影響

本物質は水溶液中で完全にイオンに解離するため、水圏からの揮発は生じにくい。媒体別

化学生物総合管理　第6巻第2号（2010.12）　180-188頁
連絡先：〒158-8501 世田谷区上用賀 1-18-1　E-mail: hirose@nihs.go.jp
受付日：2010年1月25日　　受理日：2010年6月27日

分配割合の予測の結果、本物質が水圏に放出された場合は主に水圏（99.8%）に残留する。また、本物質は容易に生分解し、魚類への生物濃縮性は低いと推定される（BCF：3.16［計算値］）。

水生生物に対する急性毒性について、魚類の半数致死濃度（LC_{50}）は 100 mg/L以上（96 時間、OECD TG 203）、ミジンコのLC_{50}は 1,000 mg/L以上（48 時間、OECD TG 202）、藻類の半数影響濃度（EC_{50}）は 1,000 mg/L以上（72 時間、生長速度法：OECD TG 201）であった。慢性毒性については、ミジンコの最大無影響濃度（NOEC）は 100 mg/L（21 日間、繁殖阻害：OECD TG 211）、藻類のNOECは 10 mg/L（72 時間、生長速度法：OECD TG 201）であった。

3）健康影響

ラットには経口投与、イヌには経口および腹腔内投与により同位体^{35}Sを含む本物質を与えたところ、速やかに吸収され、主に尿中に*p*-トルエンスルホン酸塩-^{35}Sとして排泄された。また、イヌでの血漿中半減期は 75 分であった。

ラットの単回経口投与毒性試験（OECD TG 401）において最高用量でも死亡例は認められず、LD_{50}は雌雄ともに 2,000 mg/kg bw以上であった。また、2,000 mg/kg bwで雌雄に下痢がみられた。

ヒドロトロープ類カテゴリーにおいてキシレンスルホン酸カルシウム（28088-63-3）やクメンスルホン酸ナトリウム（28348-53-0、32073-22-6）には皮膚刺激性がないとされたが、本物質はアルカリ性である（pH=9.6）ことから、眼や皮膚に刺激性を示す可能性がある。また、トルエンスルホン酸ナトリウム（オルト/メタ/パラ、12068-03-0）がモルモットで皮膚感作性を示さないことから、本物質には皮膚感作性はないとされた。

ラットに 0、100、300 または 1,000 mg/kg bw/dayの本物質を強制経口投与した 28 日間反復経口投与毒性試験（OECD TG 407）において、最高用量でも毒性影響は認められず、**反復投与毒性のNOAEL**は雌雄ともに**1,000 mg/kg bw/day**とされた。

雌雄ラットに交配前 2 週間から交配期間を含め、雄では 46 日間、雌では分娩後哺育 4 日まで、0、100、300 または 1,000 mg/kg bw/dayを強制経口投与した経口投与簡易生殖毒性試験（OECD TG 421）において、親動物では 1,000 mg/kg bw/dayで雌雄に下痢や軟便、雄に胃の境界縁における軽度な粘膜固有層の炎症性細胞浸潤および扁平上皮過形成がみられたが、生殖能および児の発生・発育については本物質投与による影響は認められず、**反復投与毒性のNOAEL**は雌雄ともに**300 mg/kg bw/day**、**生殖発生毒性のNOAEL**は**1,000 mg/kg bw/day**とされた。

細菌を用いる復帰突然変異試験およびチャイニーズ・ハムスター培養細胞を用いる染色体異常試験は S9mix の存在/非存在下で陰性であった。

4）結論と勧告

本物質は健康および環境に対して有害性が低いので、健康影響および環境影響についてともに LP と勧告された。

（2）レゾルシノール

英名 1,3-Benzenediol（108-46-3）（原案作成：ICCA 日本企業）

本文書では純度 95%以上のレゾルシノールが評価に用いられた。

1）曝露状況

本物質は接着剤、染毛剤、化粧品、医薬品の原料として使用されている。本物質は閉鎖系で製造・加工されるため、職業曝露の可能性は低いが、製品の使用により消費者曝露が生じ

化学生物総合管理　第 6 巻第 2 号（2010.12）　180-188 頁
連絡先：〒158-8501 世田谷区上用賀 1-18-1　E-mail: hirose@nihs.go.jp
受付日：2010 年 1 月 25 日　　受理日：2010 年 6 月 27 日

る。また、その使用や廃棄によって間接的に環境に放出される可能性がある。

2）環境影響

媒体別分配割合の予測の結果、本物質が大気・土壌・水圏に放出された場合は主に土壌（63.8%）と水圏（36.1%）に分布する。本物質は容易に生分解し、魚類への生物濃縮性も低いと推定される（BCF：3.16 [計算値]）。

水生生物に対する急性毒性について、魚類のLC_{50}は 26.8～100 mg/L（流水、96 時間）、40～60 mg/L（止水、96 時間）、魚類の 7 日間毒性試験（OECD TG 212 相当）ではEC_{50}（体重）は 54.8 mg/L、LC_{50}は 262 mg/Lであった。ミジンコのEC_{50}は 1.28 mg/L（止水、48 時間）、藻類のEC_{50}は 97 mg/L以上（72 時間、生長速度法：OECD TG 201）であった。慢性毒性については、魚類の 60 日間毒性試験（OECD TG 210 相当）では最小影響濃度（LOEC）は 32 mg/L（体重）、EC_{50}（胚致死/形態異常）は 260 mg/Lであり、さらに、LC_{50}は 320 mg/Lより大きいことが初期評価文書のDossierに記載されている。ミジンコのNOECは試験最高濃度の 172 μg/L（21 日間、繁殖阻害：OECD TG 211）であり、藻類のNOECは 97 mg/L（72 時間、生長速度法：OECD TG 201）であった。

3）健康影響

ラットとウサギに本物質を経口投与したところ、速やかに吸収・代謝され、尿中に排泄された。本物質をラットに反復経口投与した場合には代謝速度の増加がみられた。ヒトでの経皮吸収は緩やかだが、ラットやウサギへの経口投与と同様に代謝・排泄された。

ラットの単回経口投与毒性試験（OECD TG 401）でのLD_{50}は 510 mg/kg bwであり、毒性症状として、眼瞼下垂、呼吸器官への影響、無気力、異常歩行、振戦、けいれん、および流涎が認められた。その他の試験では、雄ラットの経口LD_{50}は 980 mg/kg bw、雌ラットのエアロゾル吸入LC_0は 7,800 mg/m^{3}以上（1 時間曝露）、2,800 mg/ m^{3}以上（8 時間曝露）であった。雄ウサギの経皮LD_{50}は 3,360 mg/kg bw、比較的純度の低い物質を用いた場合には 2,830 mg/kg bwであった。これらの急性曝露試験では中枢神経系への影響が認められた。

本物質にウサギの皮膚および眼に対する刺激性は認められなかった（OECD TG 404、TG 405、2.5%水溶液）が、溶解または半固体状態で投与したその他の試験においては、皮膚と眼に刺激性が認められた。本物質は、モルモット Maximization 試験（OECD TG 406）では中程度の、マウス LLNA 試験（OECD TG 429）では弱い皮膚感作性を示した。本物質は皮膚炎患者へのパッチテストでアレルギー反応を引き起こした。

雌雄ラットに 0、40、80 または 250 mg/kg bw/dayを週 5 日強制経口投与した 90 日間反復経口投与毒性試験（OECD TG 408）では、250 mg/kg bw/dayにおいて雌雄に間代性痙攣や流涎がみられ、雌では体重増加量の減少も認められたことから、反復投与毒性のNOAELは80 mg/kg bw/dayとされた。

ラットを用いた一連の反復強制経口投与試験（17 日間、13 週間、または、104 週間）が行われ、17 日間（用量設定）試験において 55 mg/kg bw/day以上の雌ラットに異常な興奮状態がみられたことから、一連の試験で最も低いNOAELは27.5 mg/kg bw/dayとされた。雄ラットでは 104 週間試験の最低用量 112 mg/kg bw/day以上で運動失調、腹臥位、流涎、振戦がみられ、この試験で最も低いLOAELは112 mg/kg bw/dayとされた。104 週間試験の最高用量 225 mg/kg bw/dayでは体重増加量の減少と死亡の増加も認められた。また、104 週間試験では認められなかったが、13 週間試験において絶対・相対肝重量の増加が雌では 65 mg/kg bw/day、雄では 130 mg/kg bw/dayで認められ、さらに、絶対・相対副腎重量の高値が最低用量 32 mg/kg bw/day以上の雄の生存ラットで認められた。

ラットと同様、マウスを用いた一連の反復強制経口投与試験（17 日間、13 週間、または、

化学生物総合管理　第 6 巻第 2 号（2010.12）　180-188 頁
連絡先：〒158-8501 世田谷区上用賀 1-18-1　E-mail: hirose@nihs.go.jp
受付日：2010 年 1 月 25 日　　受理日：2010 年 6 月 27 日